



# Heat Pump Rooftop Unit Demonstration

## Final Report

ET23SWE0054



Prepared by:

**Curtis Harrington, UC Davis WCEC**

**Frederick Meyers, UC Davis WCEC**

**Grant Baumgardner, Center for Energy and Environment**

**Alex Haynor, Center for Energy and Environment**

January 22, 2026

## Acknowledgements

The authors would like to thank the UC Davis Facilities department for coordinating the installation of the heat pumps, facilitating building access for WCEC researchers, and providing their feedback and guidance on the project plan.

## Disclaimer

The CalNEXT program is designed and implemented by Cohen Ventures, Inc., DBA Energy Solutions (“Energy Solutions”). Southern California Edison Company, on behalf of itself, Pacific Gas and Electric Company, and San Diego Gas & Electric® Company (collectively, the “CA Electric IOUs”), has contracted with Energy Solutions for CalNEXT. CalNEXT is available in each of the CA Electric IOU’s service territories. Customers who participate in CalNEXT are under individual agreements between the customer and Energy Solutions or Energy Solutions’ subcontractors (Terms of Use). The CA Electric IOUs are not parties to, nor guarantors of, any Terms of Use with Energy Solutions. The CA Electric IOUs have no contractual obligation, directly or indirectly, to the customer. The CA Electric IOUs are not liable for any actions or inactions of Energy Solutions, or any distributor, vendor, installer, or manufacturer of product(s) offered through CalNEXT. The CA Electric IOUs do not recommend, endorse, qualify, guarantee, or make any representations or warranties (express or implied) regarding the findings, services, work, quality, financial stability, or performance of Energy Solutions or any of Energy Solutions’ distributors, contractors, subcontractors, installers of products, or any product brand listed on Energy Solutions’ website or provided, directly or indirectly, by Energy Solutions. If applicable, prior to entering into any Terms of Use, customers should thoroughly review the terms and conditions of such Terms of Use so they are fully informed of their rights and obligations under the Terms of Use, and should perform their own research and due diligence, and obtain multiple bids or quotes when seeking a contractor to perform work of any type.

# Executive Summary

## Overview

Meeting California's ambitious energy and carbon goals will require solutions to switch the primary fuel for heating buildings from natural gas to electricity. While heat pumps have been on the market for decades, their initial and ongoing costs have thus far not been competitive with traditional natural gas furnace solutions. The focus of this project was on packaged rooftop units (RTUs) which are estimated to provide space conditioning for 75% of commercial building space in California (SCE, 2015) with most relying on natural gas for space heating. This project characterized installed heat pump RTU system performance and savings relative to a conventional baseline system for both standard and high efficiency RTUs. Installed performance data was used to recommend strategies for RTU operation that meet conditioning loads and are economically and environmentally optimized. The experience of installing retrofit RTUs was used to develop an understanding of the real-world barriers and benefits of this technology in this application. The combination of the installation experience and system monitoring results was used to provide recommendations and inform program strategy. Long term, the goal of for this project is to increase the adoption of decarbonized heating for commercial facilities and provide a better understanding of grid impacts of transitioning to electric heating sources.

## Methodology

This project monitored the performance of three RTUs to determine the impact of electrification retrofits for commercial RTUs. The team installed two heat pump RTUs on buildings on the UC Davis campus and chose one existing gas-fired RTU as a baseline. The focus of the analysis was on heating performance in the winter, but cooling season data is also presented to further demonstrate the energy performance of the retrofits. The two heat pump RTUs were installed serving two different zones in the same office building while the gas-fired RTU was installed on another office building. Monitored performance data from these three RTUs was used for both descriptive and predictive analysis. Descriptive analysis showed how each system performed in its application, highlighting differences between field performance and lab testing, as well as differences in control algorithms and configuration across units. However, uncontrolled variables, especially differences in building loads and ventilation configurations, prevented the use of descriptive analysis for direct comparison of the energy performance of the three RTUs. The predictive analysis used monitored performance data from each unit to develop models of heating and cooling performance that when applied to identical building load profiles, output expected annual energy consumption predictions for each unit that could be compared directly.

## Approach

The RTUs were monitored from October 30, 2024, through July 30, 2025, to evaluate the installed performance across a range of outdoor air conditions. Instrumentation was installed to measure capacity delivered, energy use, and controls actuators to identify operating modes. The analysis allowed annual energy consumption to be estimated for each of the RTUs and used to make recommendations for heat pump RTU installations in California. Since the study was limited to only a couple RTU manufacturers, the focus of the analysis was on specific features including variable-speed compressors, defrost strategies, and avoiding the installation of electric resistance heaters.

## Key Findings

The results showed that the high-efficiency RTU reduced heating and cooling energy consumption by 7% relative to the standard-efficiency RTU which is lower than expected considering the rated efficiency was 25% higher for the high-efficiency unit. When comparing the performance between the heat pump RTUs and the gas-fired RTU, the heat pump units demonstrated significant potential to reduce energy use, operating costs, and greenhouse gas emissions. Both heat pump RTUs showed reduction in on-site energy use and greenhouse gas emissions of more than 50% compared to the gas-fired RTU. The cost savings for the high efficiency heat pump RTU was about 10% compared to the gas-fired unit versus 3% for the standard efficiency heat pump compared to the gas-fired unit showing a cost benefit to ratepayers even when the relative cost of natural gas is low compared to electricity.

The largest difference in operation between the high-efficiency and standard-efficiency heat pump RTUs was related to their defrost strategy and peak power draw. Defrost for the high-efficiency RTU was accomplished without the need for electric resistance auxiliary heaters that reduced total energy required for defrost and peak power used. Typical defrost cycles require the unit to switch into cooling mode temporarily to defrost the outdoor coil during the heating season. The standard-efficiency RTU included a 5 kW electric resistance heater that would be used to reheat air that was cooled during the defrost cycle, whereas the high-efficiency unit shut down the indoor blower fan and used its modulating compressor to accomplish defrost without supplying cold air to the building. Evaluating the 15-minute peak power draw of both HP RTUs showed a 20% reduction in the winter for the high-efficiency unit without electric resistance heaters.

## Stakeholder Feedback

The project team has reached out to various stakeholders over the course of the project including manufacturers, contractors, CalNEXT project partners, CalMTA, and other subject matter experts. There is a keen interest in developing a better understanding of the heat pump RTU market in California, specifically related barriers to adoption and cost implications. Manufacturers and contractors have noted that removing electric resistance heaters could reduce supply air temperatures in heating season causing comfort issues, but for low outdoor air applications and mild California climates this may not be an issue. Furthermore, the advantage of avoiding adding resistance heat can remove installation barriers related to panel capacity and the cost of upgrading existing electrical infrastructure. CalNEXT and CalMTA have both expressed interest in the outcome of this study related to the implications of energy efficient features for RTUs including variable-capacity compressors and controls. The project team has also received feedback from the DOE Commercial Heat Pump Accelerator that installing heat pumps without electric resistance heaters was accomplished on several RTU retrofits on Los Angeles Unified School District campuses without issue providing confidence in that recommendation for certain California climate zones.

## Recommendations

This project demonstrated the advantages of heat pump RTUs over existing gas-fired RTUs. The heat pump equipment had lower operating costs and reduced the greenhouse gas emissions associated with space conditioning of a typical commercial office building. The high-efficiency unit showed the benefit that variable-speed compressors can have on peak power draw and ability to maintain comfort without electric resistance heaters. The standard-efficiency heat pump RTU relied on electric

resistance heaters to avoid supplying cold air in the winter during defrost cycles. Given the performance measured in this project, prioritizing heat pump RTUs that can perform defrost without electric resistance backup heat is recommended. It is expected that this will not only reduce energy costs and peak power draw but also reduce installation barriers associated with retrofit installations of heat pumps. Auxiliary heaters would likely require upgraded electrical service to the rooftop and possibly trigger a panel upgrade if the existing infrastructure cannot support the new electrical load.

## Abbreviations and Acronyms

Acronym	Meaning
ASHP	Air Source Heat Pump
BMS	Building Management Software
COP	Coefficient of Performance
COT	Coil Outlet Temperature
CT	Current Transformer
HP	Heat Pump
HVAC	Heating, Ventilation, and Air Conditioning
MAT	Mixed Air Temperature
RAT	Return Air Temperature
SAT	Supply Air Temperature
RTU	Rooftop Unit

# Table of Contents

Acknowledgements .....	ii
Executive Summary .....	iii
Overview .....	iii
Methodology .....	iii
Approach .....	iii
Key Findings .....	iv
Stakeholder Feedback .....	iv
Recommendations .....	iv
Abbreviations and Acronyms .....	vi
Introduction.....	1
Background.....	1
Objectives.....	1
Methodology & Approach.....	2
Instrumentation Plan .....	2
Test Sites and Monitoring Installation.....	7
Data Analysis .....	14
Performance Modeling .....	16
Findings .....	18
Performance Modeling Results.....	38
<b>Stakeholder Feedback</b> .....	40
Conclusions and Recommendations .....	41
References .....	43

## List of Tables

Table 1 - Datalogger Fields for RTU.....	3
Table 2 - Equipment Summary.....	4
Table 3 - Operating Mode Mapping.....	5
Table 4. Utility cost data used for the analysis .....	17
Table 5. Emissions factors used in the analysis of greenhouse gas emissions. The electrical emissions factor shown is the average, but hourly variations are used in the model. .....	17
Table 6. Data labels for each RTU in the results.....	18
Table 7. Definition of operating modes used in the analysis .....	18
Table 8. Fraction of time spent in each operating mode .....	19
Table 9. Conditioning load for spaces served by each RTU in the study .....	27
Table 10. Regression model statistics for heating.....	38
Table 11. Regression model statistics for cooling .....	39
Table 12. Normalized energy use for each RTU operating at the RTU1 site .....	39

## List of Figures

Figure 1. Heat Pump RTU instrumentation .....	4
Figure 2. Photo of existing gas-fired RTU used as a baseline for comparison .....	7
Figure 3. Thermocouples array and temperature humidity probe installed on return of gas-fired RTU .....	8
Figure 4. Data acquisition enclosure for gas-fired RTU power measurements.....	9
Figure 5. Gas-fired RTU and data acquisition enclosure for temperature, humidity, pressure, and component state measurements.....	9
Figure 6. Mechanical plans for building showing ducting layout .....	10
Figure 7. Zone map showing offices served by each zone. The pink zone shows the zone served by the	

minimum DOE efficient system while the yellow zone shows the zone served by the high efficiency unit.	10
Figure 8. Heat pump RTUs photographed during installation.....	11
Figure 9. Data monitoring enclosure.....	12
Figure 10: Return (left) and supply (right) temperature and humidity probes. ....	13
Figure 11: Mixed air plenum before the coil of the single speed HP RTU showing distributed thermocouples. (Temperature and humidity probe was also installed but not shown here).....	14
Figure 12. Standard HP RTU - Daily operating mode fraction observed during the monitoring period .....	21
Figure 13. High-Efficiency HP RTU - Daily operating mode fraction observed during the monitoring period .....	21
Figure 14. Baseline Gas-Fired RTU - Daily operating mode fraction observed during the monitoring period .....	22
Figure 15. Standard HP RTU – Operating mode fraction plotted against average daily outdoor air temperature .....	23
Figure 16. High-Efficiency HP RTU – Operating mode fraction plotted against average daily outdoor air temperature .....	23
Figure 17. Baseline Gas-Fired RTU – Operating mode fraction plotted against average daily outdoor air temperature .....	24
Figure 18. Standard HP RTU –Energy input by day and mode.....	25
Figure 19. High-Efficiency HP RTU –Energy input by day and mode.....	25
Figure 20. Gas-Fired RTU –Energy input by day and mode.....	26
Figure 21. Average input power by mode for heat pump RTUs under different outdoor conditions .....	27
Figure 22. Standard HP RTU - Net daily capacity delivered during the monitoring period.....	28
Figure 23. High-Efficiency HP RTU - Net daily capacity delivered during the monitoring period .....	29
Figure 24. Gas-Fired RTU - Net daily capacity delivered during the monitoring period.....	29
Figure 26. Standard HP RTU – Overall COP measured at different ambient temperature bins .....	30
Figure 26. COP by mode and outdoor air temperature for each RTU .....	31
Figure 27. Average COP by compressor cycle at different outdoor air temperatures for each RTU .....	32
Figure 28. Heating and cooling cycle durations measured for each RTU .....	33
Figure 29. Final supply air temperatures in heating mode for all RTUs.....	34
Figure 31. Defrosts per day at different daily average outdoor air conditions for the heat pump RTUs ....	35
Figure 31. Standard HP RTU - Average defrost duration for each stage of the defrost cycle .....	36
Figure 33. High-Efficiency HP RTU - Average defrost duration .....	36
Figure 34. Defrost cycle energy use for the heat pump RTUs.....	37
Figure 35. Standard HP RTU - Minimum supply air temperature measured during a defrost cycle .....	38

## Introduction

Meeting California's ambitious energy and carbon goals will require solutions to switch the primary fuel for heating buildings from natural gas to electricity. While heat pumps have been on the market for decades, their initial and ongoing costs have thus far not been competitive with traditional natural gas furnace solutions. Though space conditioning heat pumps are a keystone technology in California's plans to decarbonize, there are still uncertainties in the market about what heat pump technology to select for a particular application and the benefits of different features offered by heat pump products.

The focus of this project was on packaged rooftop units (RTUs) which are estimated to provide space conditioning for 75% of commercial building space in California (SCE, 2015) with most relying on natural gas for space heating. This project was aimed at understanding the potential of heat pump RTU technology to electrify and decarbonize existing commercial building heating loads. Primary data was collected on the performance of both a standard and high efficiency RTU relative to a representative gas-fired RTU. The project evaluated the implications of the different equipment on building energy use and associated costs, and carbon emissions. In addition, the project team documented the installation process and identified key features that allowed for the elimination of supplemental electric heating elements without sacrificing comfort.

## Background

Rooftop units are particularly ripe for market transformation as they are ubiquitous in the commercial sector with decades of little to no advancement and innovation. There are existing programs intended to spur adoption of heat pump RTUs but there are very few instances of these programs being utilized suggesting the uptake is still very low. Significant research and field testing have already been performed on residential applications of air-source heat pumps (ASHPs). However, the limited use of heat pumps to date in the commercial roof-top unit (RTU) market has meant that there is little available third-party data to demonstrate the performance characteristics as well as non-energy benefits of heat pump RTUs. There is an urgent need to address this gap in the available data as consumers, utilities, and governments seek ways to significantly reduce emissions from space heating in a commercial building market which has a high penetration of existing RTUs. Heat pump RTUs offer an ideal solution for existing buildings because they can be drop-in replacements for existing RTU systems, reducing installation time and cost.

## Objectives

This project characterized installed heat pump RTU system performance and savings relative to a conventional baseline system for both standard and high efficiency RTUs. Installed performance data was used to recommend strategies for RTU operation that meet conditioning loads and are economically and environmentally optimized. The experience of installing retrofit RTUs was used to develop an understanding of the real-world barriers and benefits of this technology in this

application. The combination of the installation experience and system monitoring results was used to provide recommendations and inform program strategy. Long term, the goal of for this project is to increase the adoption of decarbonized heating for commercial facilities and provide a better understanding of grid impacts of transitioning to electric heating sources.

## Methodology & Approach

This project monitored the performance of three RTUs to determine the impact of electrification retrofits for commercial RTUs. The team installed two heat pump RTUs on buildings on the UC Davis campus and chose one existing gas-fired RTU as a baseline. The focus of the analysis was on heating performance in the winter, but cooling season data is also presented to further demonstrate the energy performance of the retrofits. The two heat pump RTUs were installed serving two different zones in the same office building while the existing gas-fired RTU was located on another office building. Monitored performance data from these three RTUs was used for both descriptive and predictive analysis. Descriptive analysis showed how each system performed in its application, highlighting differences between field performance and lab testing, as well as differences in control algorithms and configuration across units. However, uncontrolled variables, especially differences in building loads and ventilation configurations, prevented the use of descriptive analysis for direct comparison of the energy performance of the three RTUs. The predictive analysis used monitored performance data from each unit to develop models of heating and cooling performance that when applied to identical building load profiles, output expected annual energy consumption predictions for each unit that could be compared directly.

## Instrumentation Plan

The instrumentation installed to monitor performance is described below and outlined in Table 1.

### Power Measurements

A power meter (eGauge 4105) was installed in the panel disconnect serving each unit to measure the power on each RTU. The eGauge devices were connected to a network using a cellular modem.

The eGauges continuously uploaded data to the eGauge server. Data at one-second intervals were retrieved from the server daily using a script that makes use of the eGauge python API. The total electrical power input of the system was calculated as the sum of the power measured on each phase.

### RTU Operating Parameters

An independent data logger (Campbell Scientific CR3000) was installed at each unit to measure temperatures and actuator statuses. Wireless communication was enabled by an expansion module, Campbell Scientific NL-241. Temperatures were measured with thermocouples, thermocouple arrays, and resistance temperature devices while HP RTU actuator outputs were measured with current transformers (CTs).

Table 1 - Datalogger Fields for RTU

Field Name	Definition	Units
<b>datetime</b>	timestamp	-
<b>rec_nbr</b>	unique ID	-
<b>sat1</b>	Supply Air Temperature 1	F
<b>sat2</b>	Supply Air Temperature 2	F
<b>rat</b>	Return Air Temperature	F
<b>mat1</b>	Mixed Air Temperature 1	F
<b>mat2</b>	Mixed Air Temperature 2	F
<b>mat3</b>	Mixed Air Temperature 3	F
<b>mat4</b>	Mixed Air Temperature 4	F
<b>oat</b>	Outdoor Air Temperature	F
<b>cot</b>	Coil Outlet Temperature	F
<b>cdt</b>	Compressor Discharge Temperature	F
<b>supfan</b>	Supply Fan Current	mV
<b>strip_heat</b>	Backup electric strip heat (if present)	mV
<b>gvalve</b>	Gas Valve Status (if present)	mV
<b>rvalve</b>	Reversing Valve Status	mV
<b>cmp</b>	Compressor Status	mV

Data at one-second intervals was transmitted from the logger to the storage server daily. Data was retrieved from the storage server on a weekly basis for processing and analysis. Sensor locations of the monitoring package are shown schematically in Figure 1.

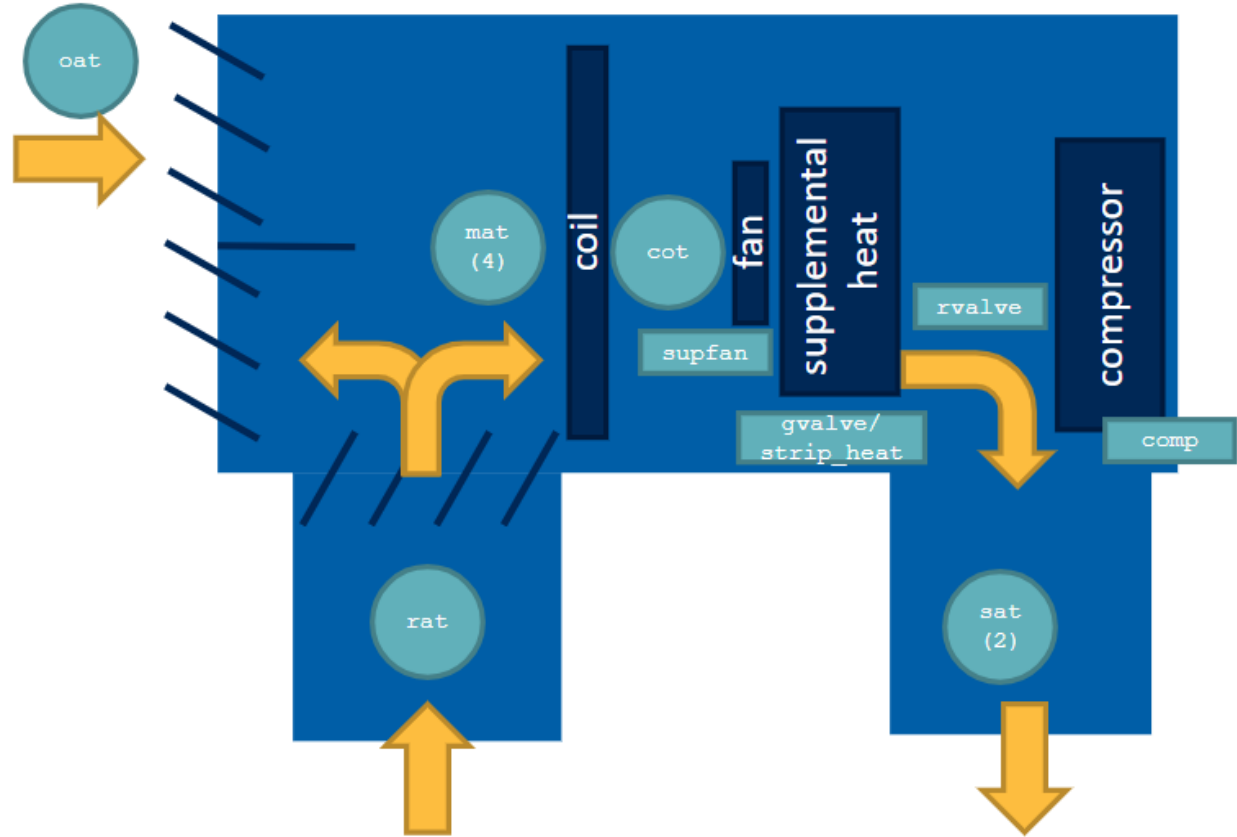


Figure 1. Heat Pump RTU instrumentation

Table 2 - Equipment Summary

Equipment	Qty
eGauge 4105	1/panel
USB-powered nano router	1/eGauge
Campbell Scientific CR3000	1/RTU
Campbell Scientific NL-241	1/RTU
current transformers	5/RTU
Cellular modem	1

## Weather Data

Outdoor temperature and humidity measured directly on each rooftop and were also collected from a nearby weather station. The primary measurements were used to correlate performance results with outdoor conditions and calculate mixed air conditions for the RTUs.

## Airflow Measurements

Airflow was characterized through a one-time measurement and correlation approach. These measurements were made by using a combination of tracer gas airflow methods and powered flow hood methods. The measurements were conducted in different modes of operation including heating, cooling, and fan-only. The tracer gas measurement involves injecting a known quantity of CO<sub>2</sub> into the airstream and measuring the CO<sub>2</sub> concentration downstream after mixing. The powered flow hood method uses a calibrated fan and capture hood to measure the airflow into the outdoor air intake while maintaining ambient-neutral pressure within the hood to avoid affecting the system pressure during the measurement. When possible, the tracer gas method was used to measure both total supply air and outdoor air fraction. For RTUs that did not have ducted returns, the powered flow hood method was used to measure the outdoor airflow directly under each mode of operation and used to calculate outdoor air fraction.

The systems tended to operate at a consistent flow in each mode except for the high-efficiency unit that would vary its fan speed during defrost cycles. For those periods when the fan speed modulated, a correlation curve between airflow and supply fan current measurements at multiple fan speeds was used to calculate airflow based on the supply fan current measured on an ongoing basis.

## Data Collection

The process for analyzing the data consisted of first combining the RTU data, power meter data, and weather data into a single table for each RTU. Then, out-of-range sensor values were removed and replaced with interpolated values. Values reported by sensors measuring the same physical value were averaged.

## Data Augmentation

Next, actuator current measurements were compared with thresholds inferred from the operating data to determine whether each actuator was on (1) or off (0) at each observation. The result was recorded in a “status” field for each actuator. The system operating mode was inferred from the combination of statuses. Depending on the unit controls, adjustments to the general mapping in Table 3 were made as necessary. Specifically, the function of the reversing valve when the actuator is de-energized can be to direct hot gas to either the indoor coil (for heating) or outdoor coil (for cooling). Also, defrost may or may not be indicated by simultaneous back-up heat and cooling operation, or may require knowledge of the fan speed to accurately identify.

Table 3 - Operating Mode Mapping

Mode	Abbreviation	Supply Fan	Compressor	Back-up Heat	Reversing Valve
Off	Off	0	-	-	-

Mode	Abbreviation	Supply Fan	Compressor	Back-up Heat	Reversing Valve
Fan Only	fan_only	1	0	0	-
Backup heat	bu_heat	1	0	1	-
Heat Pump Cool	hp_cool	1	1	0	0
Heat Pump Heat	hp_heat	1	1	0	1
Defrost	defrost	1	1	1	0

Each status was compared to its previous value to detect events, or changes in RTU state. For example, a compressor-on event was defined as any observation for which the previous compressor status was off, and the current compressor status was on. Tracked events included compressor-on events, back-up heat-on events, reversing valve on or off events, and defrost-start events. Tracking events facilitate the creation of system operating states and periods. Periods are groups of consecutive observations where the RTU is in a consistent state. For example, all observations following a compressor-on event with a compressor status equal to one (1) comprise a compressor run period. Calculating RTU performance metrics aggregated by RTU operating periods provides additional insights into equipment behavior.

## Physical Calculations

RTU performance metrics were calculated for each observation. Tracked metrics included supply volumetric airflow, heat pump delta T (temperature difference), supplemental heat delta T, heat pump heating capacity, supplemental heat heating capacity, total heating capacity, electrical power input, defrost capacity, and heat pump coefficient of performance (COP). The heat pump delta T is defined as the difference between the coil outlet temperature (COT) and the mixed air temperature (MAT). The supplemental heat delta T is defined as the difference between the supply air temperature (SAT) and the coil outlet temperature (COT). Heating capacity is the product of the volumetric airflow, physical constants, unit conversion factors, and the respective delta T. Total heating capacity is the sum of the heat pump heating capacity and the supplemental heat heating capacity.

## Adjustments

Due to the short mixing length of the RTU return air and outdoor air inlet ducts, the array of MAT sensors tended to be biased towards either the outdoor air temperature (OAT) or return air temperature (RAT). This can significantly affect the apparent COP, as the average measured MAT may differ from the physical average MAT. A tracer gas and powered flow hood airflow measurement were conducted to measure the supply air flow and outdoor air flow to validate the sensor readings. Due to the bias observed in the MAT measurements, the tracer gas measurement was used to

determine the outdoor air fraction and calculate the mixed air enthalpy from outdoor and return air properties.

### **Visualization**

Characterization plots included operating mode share by day versus time, energy consumption and capacity delivered for different modes of operation, cycle-average COP for different modes and outdoor conditions, cycle-average COP versus outdoor temperature, and defrost cycle behavior including energy consumption and frequency.

## **Test Sites and Monitoring Installation**

### **Baseline Unit**

The existing unit chosen for baseline monitoring was an RTU with gas heating rated at 36 kBtu/hr DX cooling and 49 kBtu/hr gas heating (Figure 2). It was manufactured by International Comfort Products in 2015 and uses R-410A. The unit serves four offices on the north side of a UC Davis Facilities building totaling 474 ft<sup>2</sup> and is controlled by a cloud-connected Pelican brand thermostat. This building was constructed sometime in the early 1960s and has undergone various renovations internally, but the shell has remained relatively unchanged. The RTU outdoor air intake is a fixed damper on the exposed rooftop return duct.



**Figure 2. Photo of existing gas-fired RTU used as a baseline for comparison**

Since the outdoor air intake is several feet upstream from the unit, the air is expected to be well mixed by the time it reaches the unit which simplifies the measurement for mixed-air conditions. Still, researchers installed an array of four thermocouples in addition to a Vaisala temperature and humidity sensor at the return intake for the gas-fired RTU (Figure 3). This array indicates if the air is well mixed, and if not, an average can be used to estimate the state of the mixed air. In addition, the tracer gas method was used to directly measure the return, supply, and outdoor air flow rates. Using both an array of sensors and the tracer gas measurement, researchers ensured an accurate assessment of the outdoor air fraction.



**Figure 3. Thermocouples array and temperature humidity probe installed on return of gas-fired RTU**

In addition to the mixed air, the properties of return air and supply air were also recorded using Vaisala HMP110 probes. The refrigerant suction, discharge, evaporator, and condenser coil temperatures were recorded using insulated surface-mount T-type thermocouples. Dwyer current transducers were also used to monitor the current draw of the compressor and supply fans. Finally, the power of the whole unit was recorded using an EGauge EG4015 energy monitor. Figure 4 and Figure 5 show the data acquisition systems installed for the gas-fired RTU.



**Figure 4. Data acquisition enclosure for gas-fired RTU power measurements**



**Figure 5. Gas-fired RTU and data acquisition enclosure for temperature, humidity, pressure, and component**

state measurements

### Heat Pump RTUs

On another office building, the two RTUs were replaced with two new heat pump RTUs. The two new heat pump RTUs were installed in October 2024, each serving a separate zone in the office building. Figure 6 and Figure 7 show the ducting layout and zone configuration for the two units.

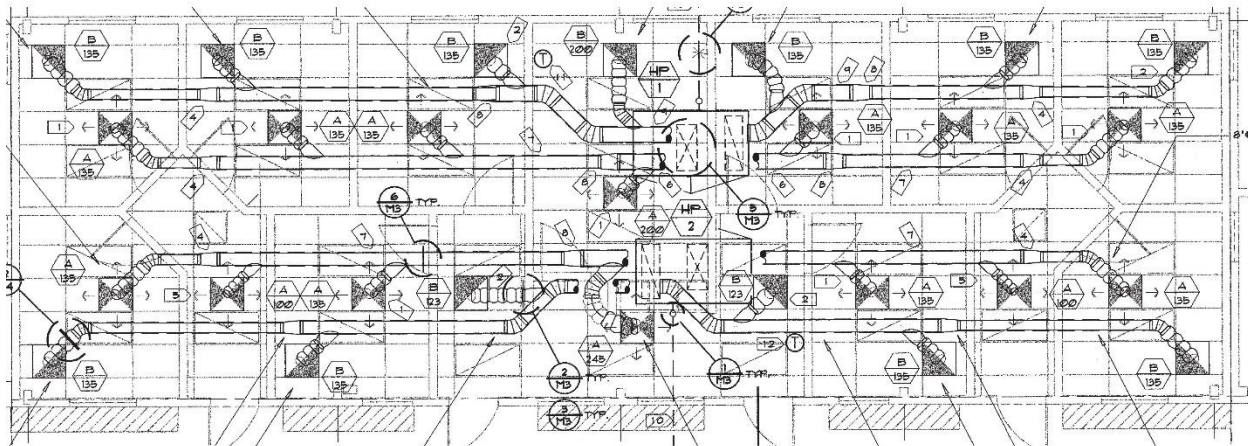


Figure 6. Mechanical plans for building showing ducting layout

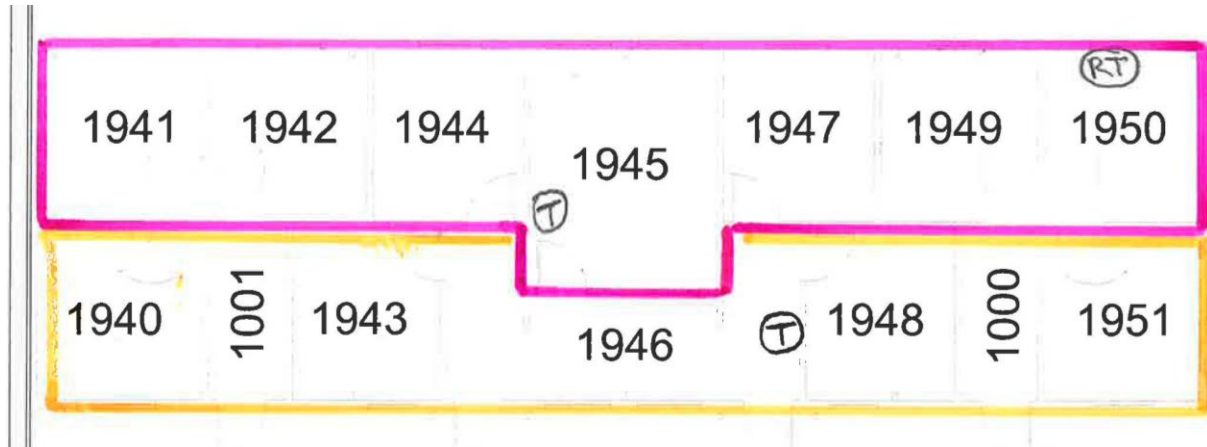


Figure 7. Zone map showing offices served by each zone. The pink zone shows the zone served by the minimum DOE efficient system while the yellow zone shows the zone served by the high efficiency unit.

The installation required mechanical, electrical, and plumbing trades to complete. The coordination of these trades delayed the installation as the electrician was unavailable for several weeks. While the electrical system was adequate to serve the heat pumps, the existing 3-phase wiring needed to be retrofitted for the 1-phase systems. Many smaller commercial RTUs (<5.4 Tons) offer options for either 3-phase or 1-phase so this step may not be needed in other installations. The plumbing contractor connected the condensate to the roof drain. The mechanical contractor mounted the unit to the existing roof curb and commissioned the unit. A curb adapter was required to mount the new RTUs on the existing roof curb. This is common for new RTU installations, even when replacing the

unit with a product from the same manufacturer. The high efficiency unit is taller with a narrower footprint than the standard efficiency unit (Figure 8).



**Figure 8. Heat pump RTUs photographed during installation**

The units were connected to a building management software (BMS) that is used to control various features including demand control ventilation, schedules, and setpoints. This software communicates with the RTUs using standard 24 VAC signals, however, more sophisticated heat pumps often rely on a digital communication protocol between their native thermostat and the RTU. This presents challenges with integrating with third-party BMS systems. The more efficient RTU includes variable-speed technology and uses a proprietary thermostat to control building setpoint. The communicating thermostat can observe the building temperature change rate and use that information to adjust operating speed. Alternatively, the unit can operate with traditional 24 VAC thermostat signals, but this would impact its approach for modulating capacity as it would not have any information about the space temperature with respect to setpoint. It was decided to allow the proprietary thermostat to control the unit during commissioning but was switched to the BMS thermostat due to the lack of specific features in the thermostat. Specifically, the thermostat did not offer a heat/cool mode to allow the thermostat to operate between a setpoint band. The lack of this feature meant that the thermostat had to be physically changed from heating to cooling modes depending on the load, and there were many periods when both heating and cooling were needed on

the same day. In addition, there was no scheduling feature in the thermostat. The BMS allowed the new RTU to be centrally controlled with the other units on the building.

For the variable-speed HP, temperature and humidity probes were installed in the return and supply. However, mixed air sensors were not installed since the geometry of the unit did not allow for good mixing before the coil. Additionally, there was no outdoor air intake on the high efficiency unit since it's primarily marketed for residential applications. A fixed damper outdoor intake was installed by UC Davis facilities but needed to be fabricated. Figure 9 through Figure 11 show the data logging enclosure and example sensor placement.



**Figure 9. Data monitoring enclosure**



**Figure 10: Return (left) and supply (right) temperature and humidity probes.**

To determine the state of heating, cooling, or defrost a current transducer was added to the refrigerant reversing valve. The current measured turned out to be very small, so the team also added thermocouples before and after the outdoor coil of the refrigerant piping to monitor the state of the system.

Current transducers were also added to the compressor and supply fan to monitor status and operating speed (0-100%). In addition, the supply fan current was mapped to the airflow measured using the tracer gas airflow measurement tool.

The single speed HP was instrumented in a similar way, except four sensors were added to the mixed air before the coil (Figure 11). While the geometry of this unit allowed for sufficient mixing to use the average of the four sensors to determine outdoor air fraction, the analysis relied on the tracer gas measurements to align with the method used on the other RTUs.



**Figure 11: Mixed air plenum before the coil of the single speed HP RTU showing distributed thermocouples. (Temperature and humidity probe was also installed but not shown here)**

## Data Analysis

Data from the data loggers was retrieved from the storage server and manipulated to calculate performance metrics and plots on a weekly basis. The analysis process generally consisted of an importing step, a calculation step, and a visualization step.

### Import Data

The data import process consisted of several steps to check for new unit or power meter data and load any files that were not yet processed. Once the latest field data was loaded, data from the two loggers were joined based on the timestamp. Next, data from local weather data was imported to the latest available date, interpolated to one-second resolution, and joined to the other field data. This independent temperature measurement helped verify site measurements. Basic processes such as renaming fields for consistency and checking for out-of-range values also occurred in this step.

## Performance Metric Calculations

There were many interesting performance metrics that were derived from the field data. At a high level, the most important metrics were overall energy input, total delivered heating and cooling capacity, and overall efficiency.

Power meter measurements were numerically integrated with respect to time to determine energy input. For the two heat pump RTUs, there was no gas input, so the power meter measurements represented all energy consumed by these units. For the gas unit, electrical power was measured in the same way, but gas flow was measured with a flow meter and used along with the gas valve actuator status to monitor gas usage. Total gas energy input was calculated by numerically integrating the gas input rate with respect to time. The total energy input was the combination of the electrical energy input and the gas energy input.

Total delivered capacity was calculated as the product of the airflow, as calculated by one-time tracer gas measurements and correlated with supply fan current, and the enthalpy difference between the mixed air to supply air. The mixed air enthalpy was calculated based on the measured outdoor air enthalpy, return air enthalpy, and outdoor air fraction as shown in the equation below. The outdoor air fraction was also determined during the one-time tracer gas or powered flow hood measurement for each mode of operation. Enthalpy was calculated from the temperature/RH probes.

$$h_{mix} = [h_{return} * (1 - OAF) + h_{outdoor} * (OAF)]$$

Where,

$$h_{mix} = \text{mixed air enthalpy (Btu/lb)}$$

$$h_{return} = \text{return air enthalpy (Btu/lb)}$$

$$h_{outdoor} = \text{outdoor air enthalpy (Btu/lb)}$$

$$OAF = \text{outdoor air fraction}$$

The efficiency, or COP of these RTUs is simply the ratio of the output capacity to the input power and calculated using the equation below. The absolute value of the output capacity was used to ensure a positive COP in both cooling and heating. The COP was only calculated as a non-zero value if the compressor was on as determined by comparison of the compressor CT to a threshold. In addition, the COP was assumed to be zero whenever the input power was zero to avoid numerical issues resulting from division by zero.

$$COP = \frac{\dot{m}_{air} * |h_{supply} - h_{mix}|}{P}$$

Where,

$$\dot{m}_{air} = \text{mass flow rate of supply air (lb/h)}$$

$$h_{supply} = \text{supply air enthalpy (Btu/lb)}$$

$$h_{mix} = \text{mixed air enthalpy (Btu/lb)}$$

$$P = \text{Power (Btu/h)}$$

These primary metrics were visualized at different aggregations (e.g., by day, or by outdoor temperature bin) to uncover additional detail.

## Compare Energy Performance

The primary performance metrics were used to develop models of RTU performance for predictive analysis. Annual energy and emissions for each RTU were estimated and compared by applying the normalized performance data to representative building load profile for the region. A regression model for each RTU was developed to predict energy use based on variables such as outdoor air temperature, mixed air temperature, and mixed air humidity.

## Additional Performance Metrics

Additional metrics beyond energy, capacity, and efficiency were useful to describe performance issues that are unique to heat pump RTUs. Relative to conventional RTUs, there are additional operating modes such as defrost and supplemental heating that significantly impact occupant comfort and utility bills. The following metrics were evaluated to more fully characterize the performance of these RTUs:

- Operating mode fractions (overall, by day, and by binned outdoor temperature)
- Average power (by operating mode and by binned outdoor temperature)
- COP versus outdoor temperature by compressor cycle
- Heating and Cooling Loads versus outdoor temperature
- Supply air temperature versus outdoor temperature
- Distributions of heat pump cycle durations
- Supplemental heating frequency and duration
- Defrost frequency and duration

Individual rows of data were labelled with an assumed operating mode based on combinations of actuator statuses in that row. For example, when the supply fan was on, the compressor was on, and the reversing valve directed hot refrigerant to the indoor coil, the RTU was in heat pump heating mode. Individual compressor and other actuator cycles were determined by identifying changes in actuator statuses from off to on with a form of timeseries edge detection. All observations between rising and falling edges belong to the same actuator cycle.

The frequency of certain modes and mode durations were estimated by flagging changes in operating modes and/or actuator statuses and assigning a unique label to each group of observations that occurred between changes in modes. Aggregating the data by this unique label allowed the duration of each occurrence of each mode to be quantified. Aggregating the data by different intervals of time and counting the number of unique mode groups in each aggregation allowed the frequencies of each mode to be quantified.

## Performance Modeling

Measured HVAC energy use often varies significantly between the different RTUs tested due to factors such as equipment efficiencies, varying building loads, ventilation controls, and thermostat setpoints. Performance modeling was conducted to better compare the impact of the retrofits without uncertainties related to uncontrolled variables in the field.

Regression models for each RTU were applied to an Energy Plus prototype model for a strip mall retail building developed by Pacific Northwest National Laboratory. The building loads were modeled for California climate zone 12 which is the same as the demonstration location. This allowed for direct comparison of annual energy use and greenhouse gas emission related to the products tested. This analysis does not include fan energy used for ventilation when not in heating and cooling modes since those controls differed between the units monitored in the field evaluations. Utility costs were based on the average price reported by the U.S. Energy Information Agency for the California Commercial end-use sector. The utility costs used in this analysis are shown in Table 4<sup>12</sup>.

**Table 4. Utility cost data used for the analysis**

	<b>Electricity (\$/kWh)</b>	<b>Gas (\$/therm)</b>
<b>Rate Used</b>	\$ 0.23	\$ 1.70

The GHG emissions data used in this analysis came from the National Renewable Energy Laboratory Cambium database<sup>3</sup> for the California region and is summarized in Table 5. The Cambium data set includes hourly and seasonal variations in emissions from power generation, which are then applied to the modeled energy use to obtain CO<sub>2</sub>e. For natural gas use, a conversion factor of 11.70 lb CO<sub>2</sub>e/therm was used based on data from the California Air Resources Board<sup>4</sup>, which provides a weighted average of emissions for natural gas.

**Table 5. Emissions factors used in the analysis of greenhouse gas emissions. The electrical emissions factor shown is the average, but hourly variations are used in the model.**

<b>Emissions Source</b>	<b>Factor</b>	<b>Units</b>
<b>NREL Cambium Data Set Emission Factor for Electricity (average)</b>	0.7034	lb CO <sub>2</sub> e /kWh

<sup>1</sup> Gas rate source: [https://www.eia.gov/dnav/ng/ng\\_pri\\_sum\\_dcu\\_sca\\_m.htm](https://www.eia.gov/dnav/ng/ng_pri_sum_dcu_sca_m.htm)

<sup>2</sup> Electricity rate source: [https://www.eia.gov/electricity/monthly/epm\\_table\\_grapher.php?t=epmt\\_5\\_6\\_a](https://www.eia.gov/electricity/monthly/epm_table_grapher.php?t=epmt_5_6_a)

<sup>3</sup> GHG emissions data for electricity: <https://www.nrel.gov/analysis/cambium>

<sup>4</sup> GHG emissions data for natural gas: [https://www.google.com/url?client=internal-element-cse&cx=009910126870644753977:9bvyj8tzpbo&q=https://ww2.arb.ca.gov/sites/default/files/auction-proceeds/cci\\_emissionfactordatabase.xlsx&sa=U&ved=2ahUKEwj08r65hKuBAXVqLUQIHUJ9A280FnoECAYQAO&usg=AOvYaw16q22CL4WsSiS45BT2wStF](https://www.google.com/url?client=internal-element-cse&cx=009910126870644753977:9bvyj8tzpbo&q=https://ww2.arb.ca.gov/sites/default/files/auction-proceeds/cci_emissionfactordatabase.xlsx&sa=U&ved=2ahUKEwj08r65hKuBAXVqLUQIHUJ9A280FnoECAYQAO&usg=AOvYaw16q22CL4WsSiS45BT2wStF)

Emissions Source	Factor	Units
Natural Gas GHG Emission Factor	11.70	lb CO <sub>2</sub> e/therm

## Findings

The results are provided for each of the three RTUs monitored for the project. Performance data collection was active for all RTUs on October 30, 2024, and continued through July 30, 2025. For simplicity in the plots, the RTUs were labeled as outlined in Table 6.

Table 6. Data labels for each RTU in the results

RTU Description	Data Label Used
Standard Efficiency Heat Pump RTU	RTU1
High Efficiency Heat Pump RTU	RTU2
Gas-fired RTU	RTU3

### Overall Mode Share

The RTUs in the study had several modes of operation including Off, Fan Only, Heat Pump Heating, Heat Pump Cooling, Defrost, Post-defrost, Auxiliary Heat, and Gas Heat. Each of these modes are defined in Table 7.

Table 7. Definition of operating modes used in the analysis

Mode	Description
Off Mode	RTU in standby mode with minimal energy used for powering electronics
Fan Only	Fan operating to provide ventilation or additional capacity following a heating or cooling cycle
HP Heat	Fan and compressor operating in heating mode

Mode	Description
HP Cool	Fan and compressor operating in cooling mode
Defrost	Various components operating to defrost the outdoor coil
Post-Defrost	Mode for standard efficiency RTU that was consistently observed at the end of a defrost period when the unit would transition to HP + Aux. Heat mode for a short period. This was distinguished from other HP + Aux. Heat instances since it was related to the defrost cycle.
Aux. Heat/Gas Heat	Fan and electric heater or gas furnace operating in heating mode
HP + Aux. Heat	HP Heat mode and electric heater operating in heating mode

Table 8 presents the time each RTU spent in a particular mode of operation during the heating season. Issues with the monitoring system resulted in some data gaps during the monitoring period which are quantified by the Data Coverage metric that describes fraction of time during the monitoring period that complete data were recorded. For the heat pump RTUs, the units spent most of the time in Fan Only mode which was during occupied periods when ventilation without heating or cooling was required. This was followed by the Off mode representing 29-37% of the time during the monitoring period. The baseline gas RTU showed very different results due to the way the unit was commissioned on the building. The gas unit was not scheduled to run in fan-only mode during occupied periods, which led to the majority of the time being spent in the Off mode representing 91% of the monitored data.

**Table 8. Fraction of time spent in each operating mode**

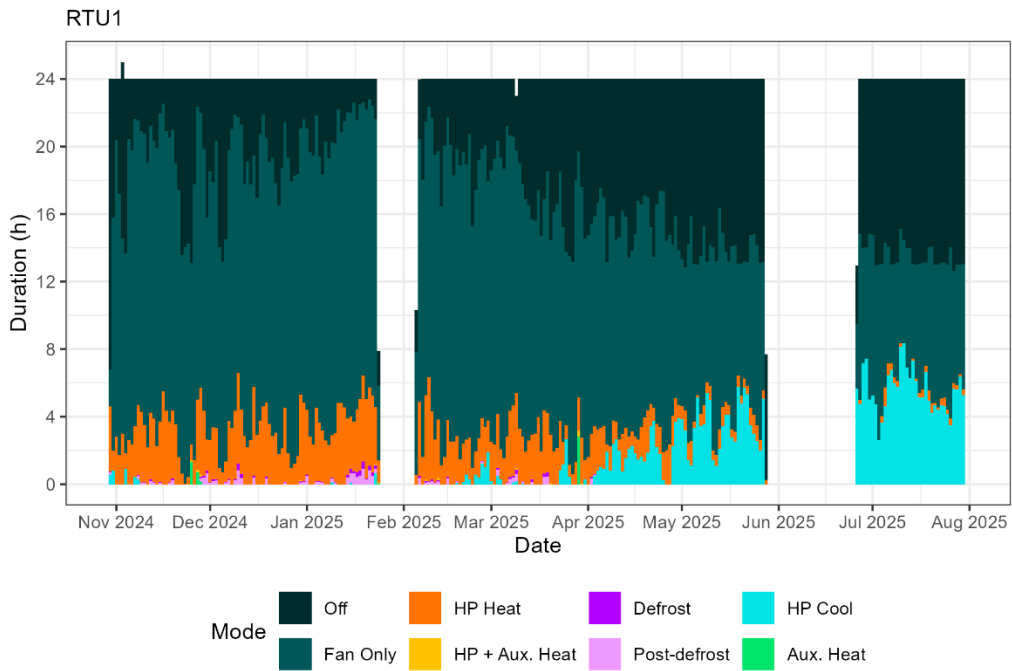
	RTU1	RTU2	RTU3
Start Date	10/30/2024	10/22/2024	09/30/2024
End Date	07/30/2025	07/30/2025	07/30/2025
Observed Hours	5583	5747	7131

	RTU1	RTU2	RTU3
Data Coverage	84.9%	84.9%	98.1%
Off Mode	28.8%	37.1%	90.6%
Fan Only	55.7%	44.3%	3.0%
HP Heat	8.7%	13.5%	-
HP Cool	6.4%	4.9%	3.0%
Defrost	0.1%	0.3%	-
Post-defrost	0.3%	-	-
Aux. Heat/Gas Heat	0.1%	-	3.4%
HP + Aux. Heat	0.03%	-	-

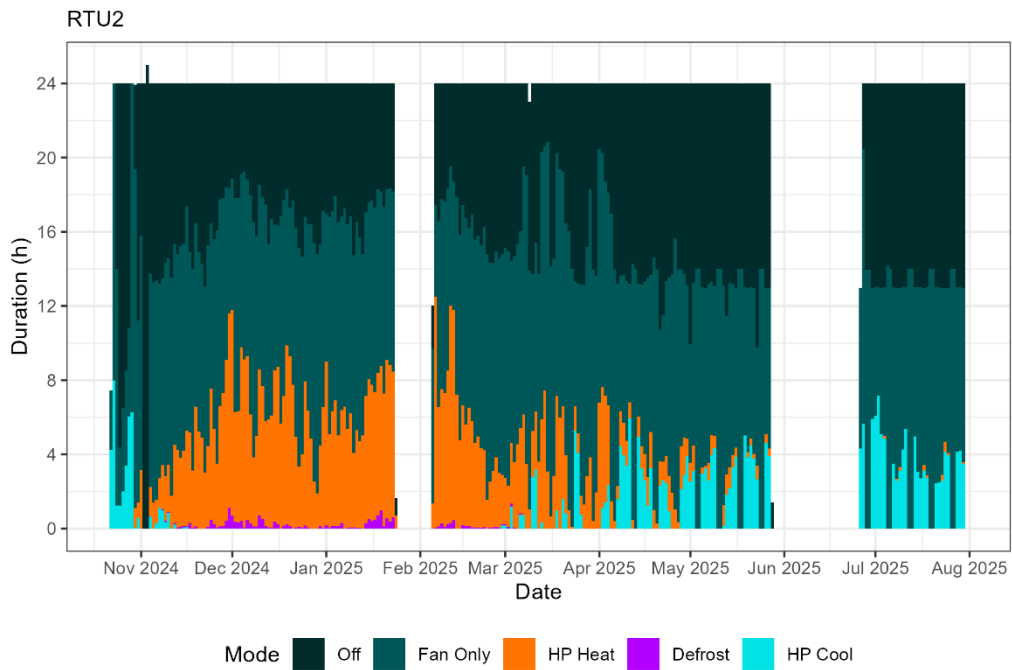
### Mode Share by Day

Figure 12 through Figure 14 show the duration of time the RTUs spent in each operating mode for each day of the monitoring period, except where power interruptions to the data loggers resulted in gaps in data. The y-axis shows the number of hours each day the units spent in each operating mode. For example, Figure 12 shows that in January RTU 1 would spend between 0-1 hour each day in Defrost, 2-6 hours each day in Heating mode, 15-18 hours each day in Fan-Only mode, and 1-5 hours each day in OFF mode. Over the course of the monitoring period, the share of each day the RTUs spend in heating or cooling modes varies according to outdoor temperatures, with 2 – 12 hours per day of heating in winter months transitioning to 1 – 4 hours per day of mixed heating and cooling in the spring, and finally 2 – 8 hours per day of cooling in the summer, depending on the RTU. The plots show that the high-efficiency heat pump had much longer heating runtimes since the compressor can run at part load. The standard efficiency heat pump and baseline gas unit are both single speed, but the gas unit showed lower heating hours due to the higher heating capacity. These plots also highlight differences in settings between units as well as changes in control settings over time. For example, Figure 14 shows that the operating mode fractions varied periodically by day. Further investigation revealed that the days with very low heating or cooling operation corresponded

to weekend days. Figure 13 shows a new periodicity in operation beginning in late March 2025 that was confirmed to be due to the introduction of a weekend thermostat setback.



**Figure 12. Standard HP RTU - Daily operating mode fraction observed during the monitoring period**



**Figure 13. High-Efficiency HP RTU - Daily operating mode fraction observed during the monitoring period**

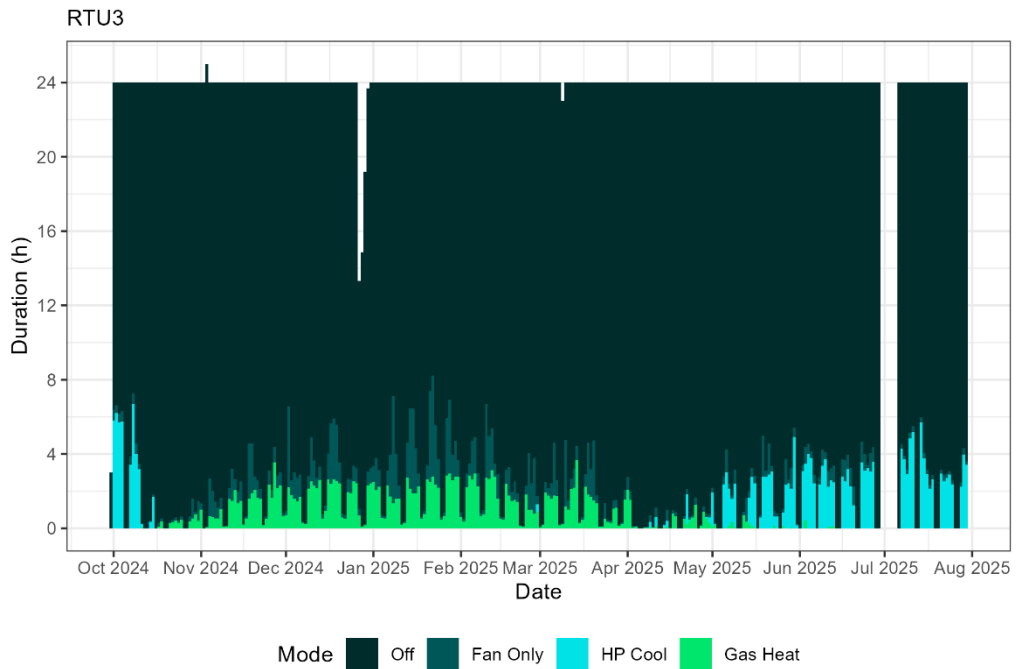


Figure 14. Baseline Gas-Fired RTU - Daily operating mode fraction observed during the monitoring period

### Mode Share by Outdoor Temperature Bin

Figure 15 through Figure 17 show similar data as the fraction of time spent in each operating mode but instead plotted against outdoor air temperature bins. These plots more clearly show the relationship between outdoor air temperature and time spent in heating or cooling modes. When conditions are cold outside, the units spend more time in heat pump heating mode and when conditions are hot the units operate more in cooling mode. The standard heat pump RTU operated significantly more in cooling mode than the high efficiency heat pump RTU and the gas-fired RTU, whereas the high efficiency RTU operated significantly more in heating mode than the other two units. The gray line on these plots shows the total hours observed in each temperature bin for each unit, as read from the secondary y-axis on the right side of the plot. This helps emphasize the relative frequency of each temperature bin during the monitoring interval.

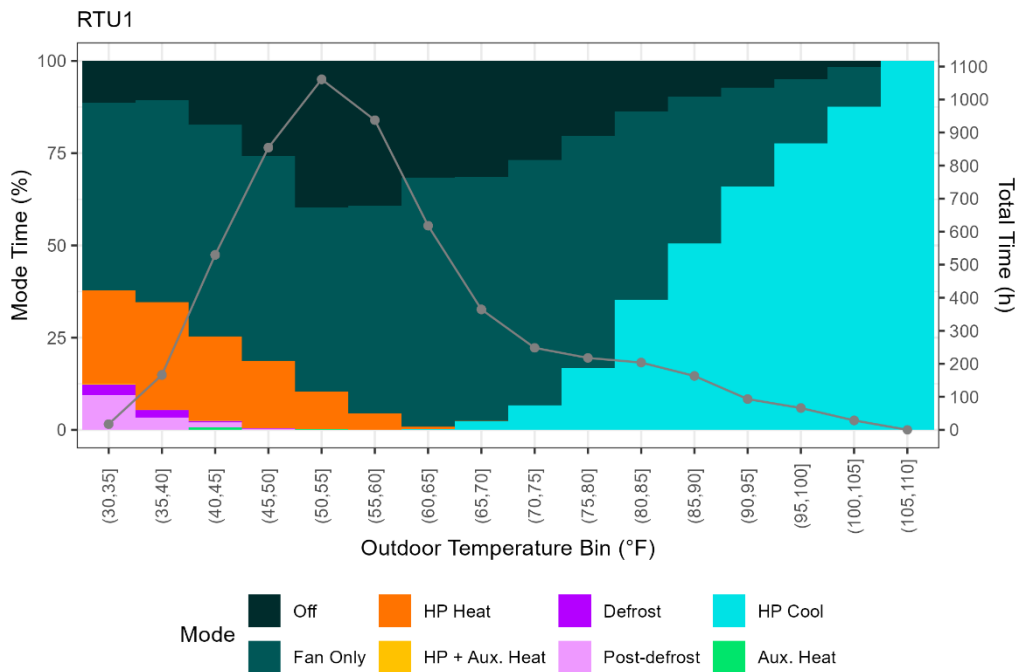


Figure 15. Standard HP RTU – Operating mode fraction plotted against average daily outdoor air temperature

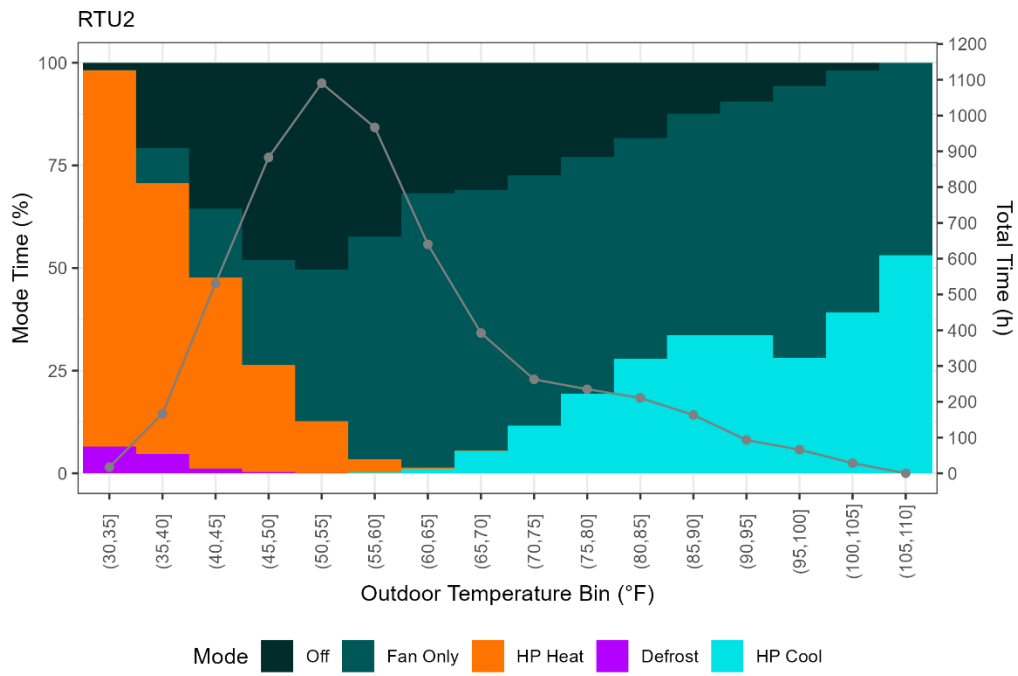
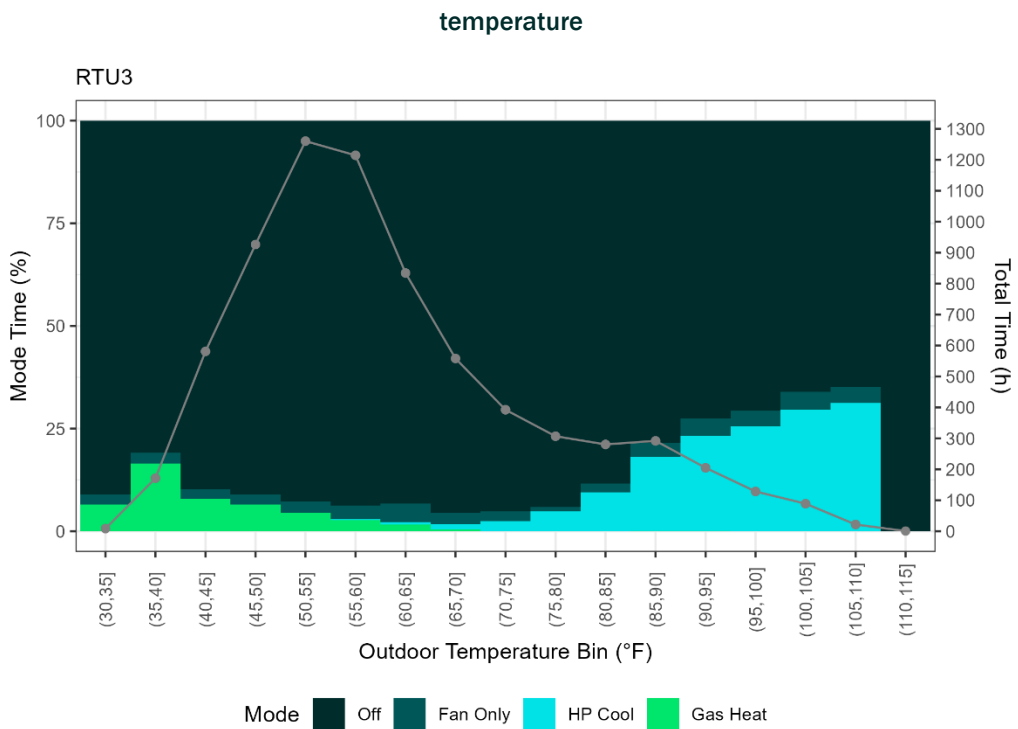


Figure 16. High-Efficiency HP RTU – Operating mode fraction plotted against average daily outdoor air



**Figure 17. Baseline Gas-Fired RTU – Operating mode fraction plotted against average daily outdoor air temperature**

### Energy Input by Day and Mode

Figure 18 through Figure 20 show the total energy input for the RTUs for each day of the monitoring period. The energy use for the standard efficiency RTU ranged from 2-24 kWh on occupied days. The lower energy use was observed on mild temperature days with energy peaks occurring on the coldest days. Interestingly, the high-efficiency RTU showed higher daily energy use reaching a peak of over 38 kWh during the heating season. In the cooling season, however, the high efficiency RTU showed lower daily average energy use than the standard efficiency RTU. This discrepancy can be at least partially attributed to differences in the heating loads in the spaces served (see Space Design Loads). To account for the differences in delivered capacity, the efficiency (COP) of each unit in each mode is calculated and shown in Figure 26. The gas unit shows daily energy use exceeding 75 kWh (converting gas thermal energy used on-site to kWh) highlighting the efficiency benefit of using a heat pump for heating over natural gas.

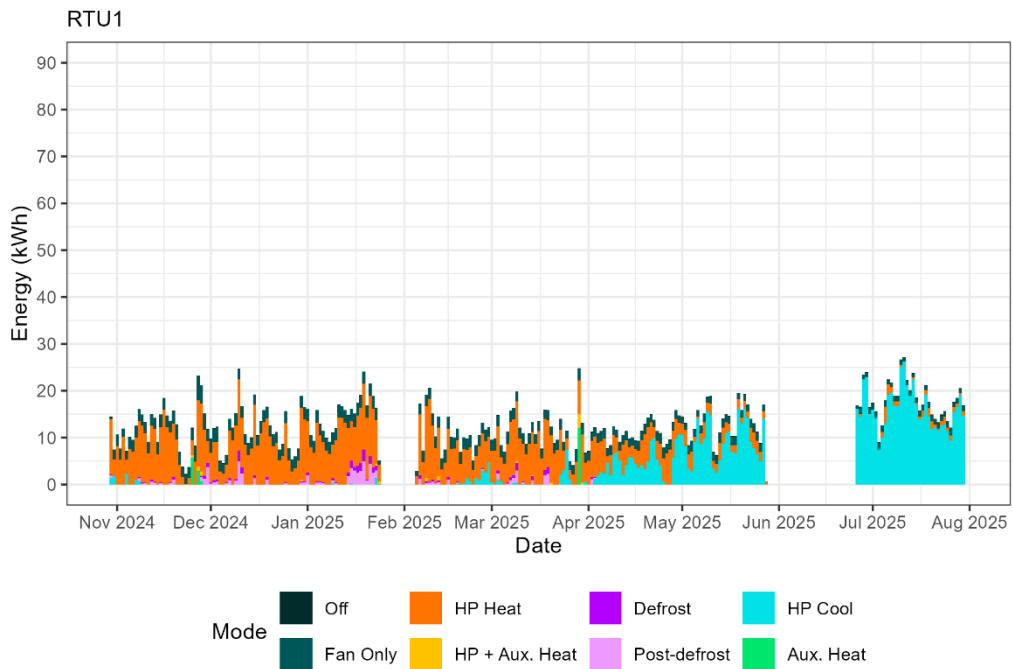


**Figure 18. Standard HP RTU –Energy input by day and mode**

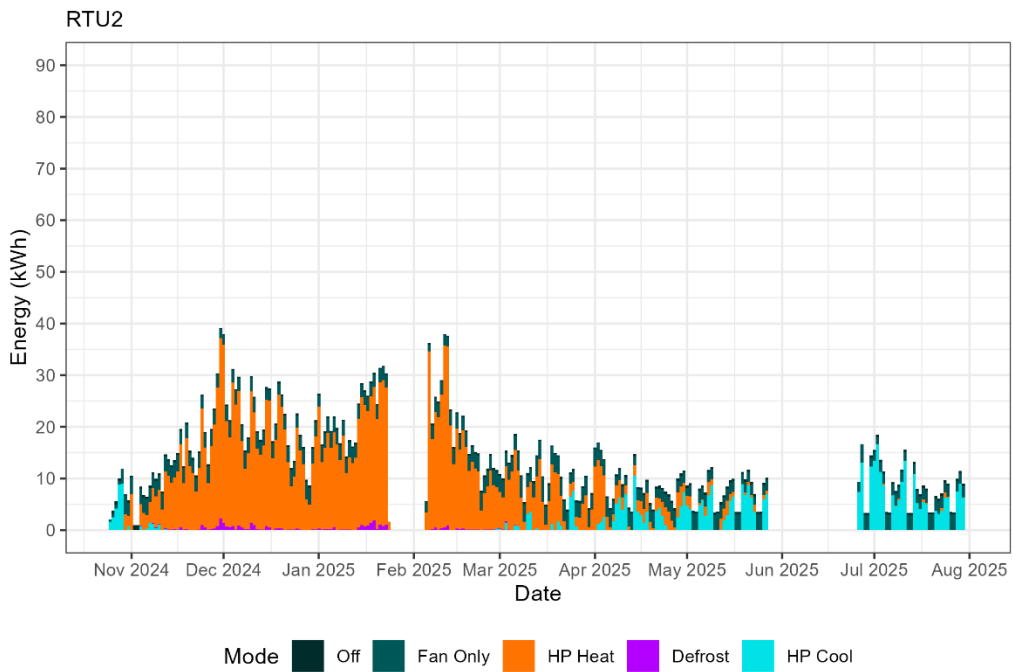


**Figure 19. High-Efficiency HP RTU –Energy input by day and mode**

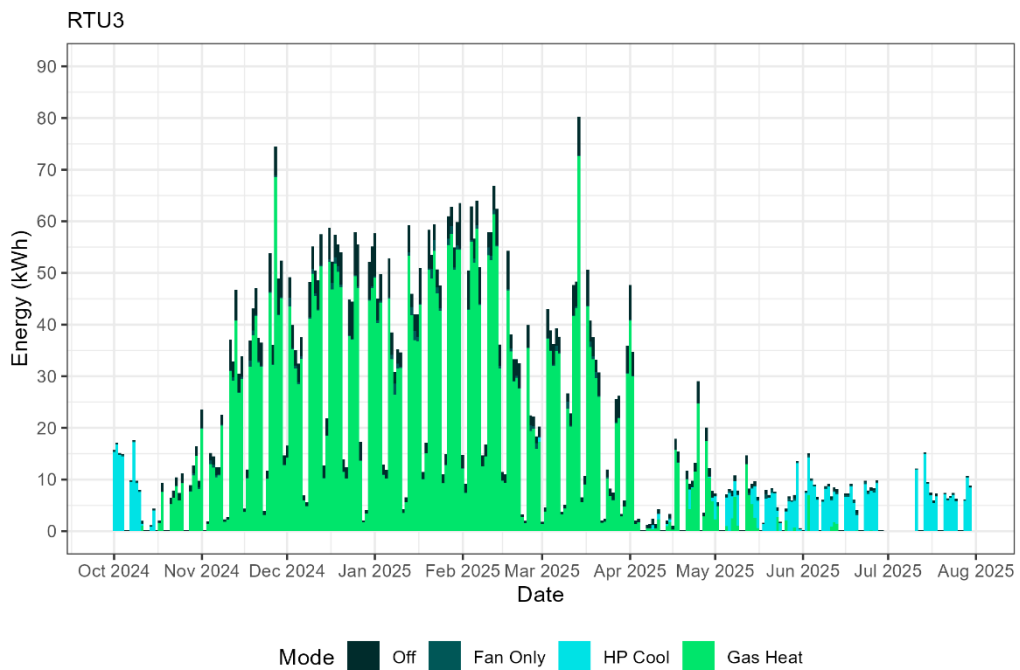


Figure 20. Gas-Fired RTU –Energy input by day and mode

### Average Power by Mode and Outdoor Temperature Bin

Figure 21 shows the average power draw of the heat pump RTUs for each operating mode under different outdoor conditions. The defrost mode for the standard efficiency RTU showed high power draw with about 5.5 kW of power used during defrost. The heat pump heating and cooling modes showed a much lower power draw at 2.3 kW to 3 kW. The variable speed capability of RTU2 appears on this plot as a wider range of power input values for heat pump heating and cooling relative to RTU1. Heat pump power input for RTU2 ranged from 1.1 kW - 3.9 kW. Higher power input is used at extreme outdoor temperatures to increase compressor speed and therefore heating or cooling capacity. The defrost strategy employed by RTU2 allowed it to use significantly less power for defrost than RTU1. The gas RTU, which was not included in Figure 21, showed a relatively consistent combined gas and electricity energy input rate of around 19 kW when in heating mode.

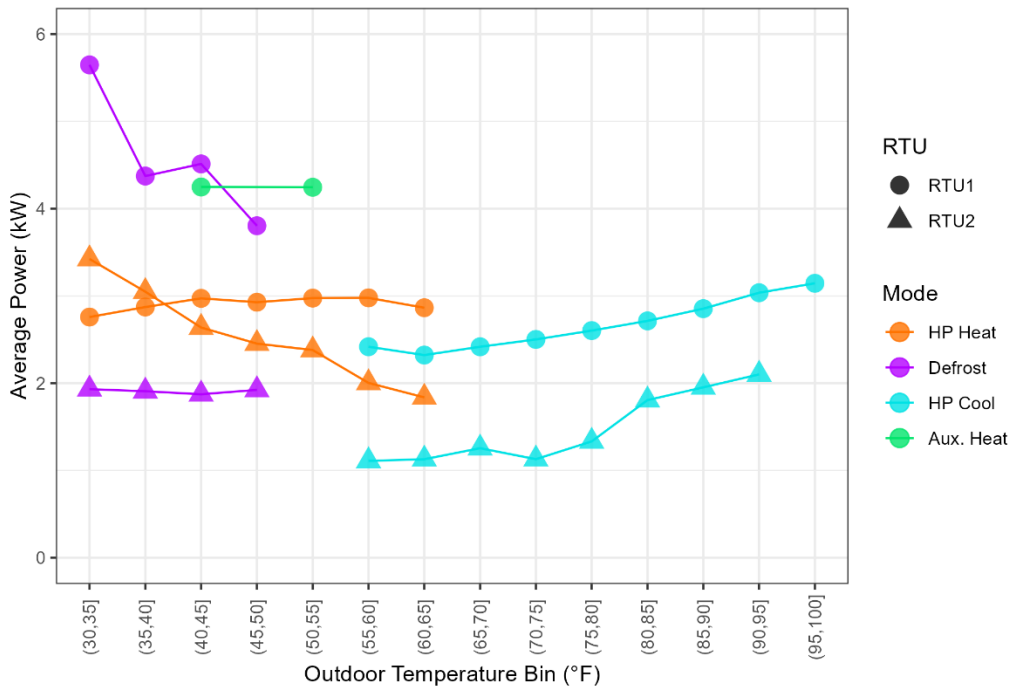


Figure 21. Average input power by mode for heat pump RTUs under different outdoor conditions

### Space Design Loads

Table 9 shows the conditioning load for the spaces served by the RTUs. The conditioning load was highest for the high-efficiency RTU followed by the standard efficiency RTU and the gas-fired RTU. This could account for the higher daily energy use observed for the high-efficiency RTU since the heating load at 30°F is over 30% higher than the conditioning load for the standard efficiency RTU.

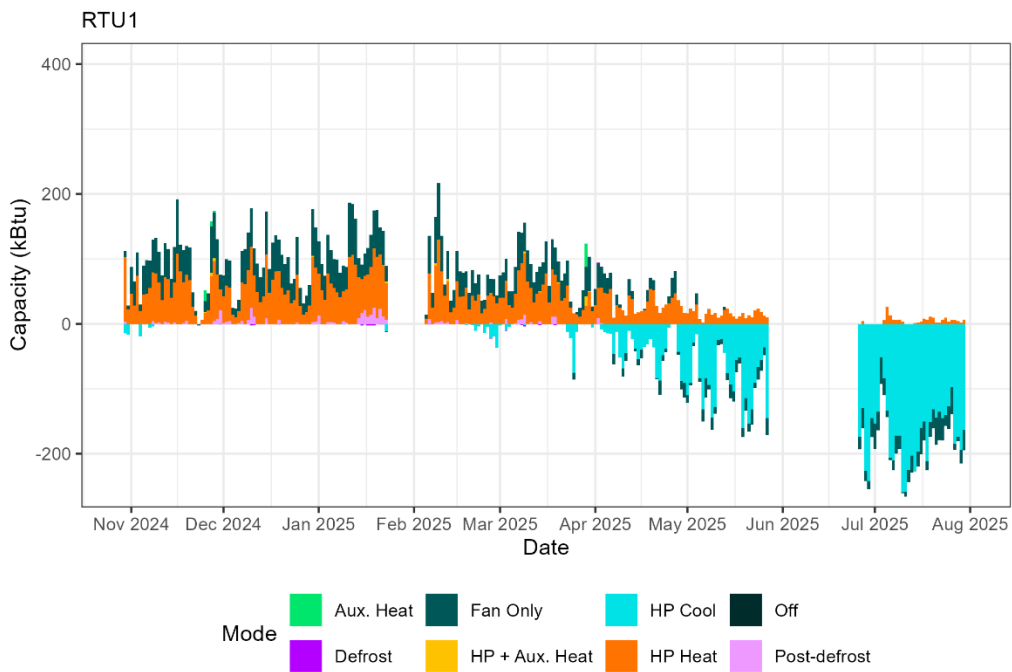
Table 9. Conditioning load for spaces served by each RTU in the study

RTU	Intercept (Btu/h)	Slope (Btu/h-°F)	Load @ 30°F (Btu/h)
RTU1	25257	-418.32	12,707
RTU2	31599	-490.60	16,881
RTU3	19162	-298.47	10,208

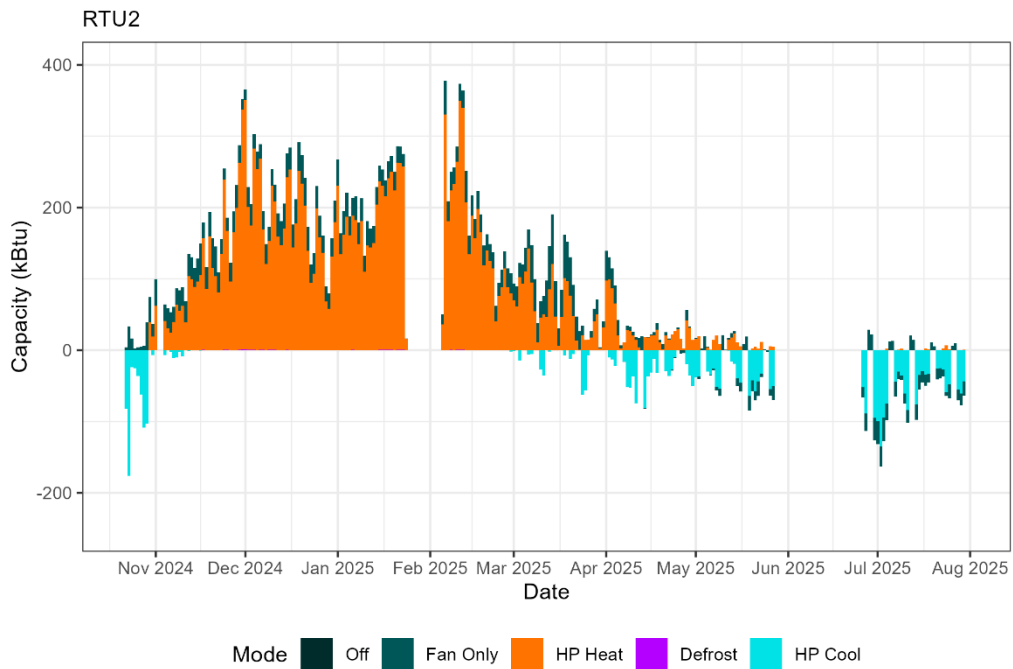
### Net Energy Output by Day and Mode

Figure 22 through Figure 24 show the net capacity delivered to the space by the RTUs during the monitoring period. These plots show more heating capacity delivered when outdoor temperatures are colder and more cooling capacity (shown as a negative value) delivered when outdoor

temperatures are hotter. Like earlier plots of daily average energy use, the capacity delivered by the standard HP RTU was lower for the heating season and higher for the cooling season compared to the high-efficiency HP RTU. The net cooling capacity delivered by the standard unit was twice the net capacity delivered by the high-efficiency unit, whereas in heating season, the net capacity of the standard unit was about half of that for the high efficiency RTU. This demonstrates the importance of monitoring both capacity and power to calculate efficiency, since space conditioning loads differ significantly between two units on the same building.



**Figure 22. Standard HP RTU - Net daily capacity delivered during the monitoring period**



**Figure 23. High-Efficiency HP RTU - Net daily capacity delivered during the monitoring period**

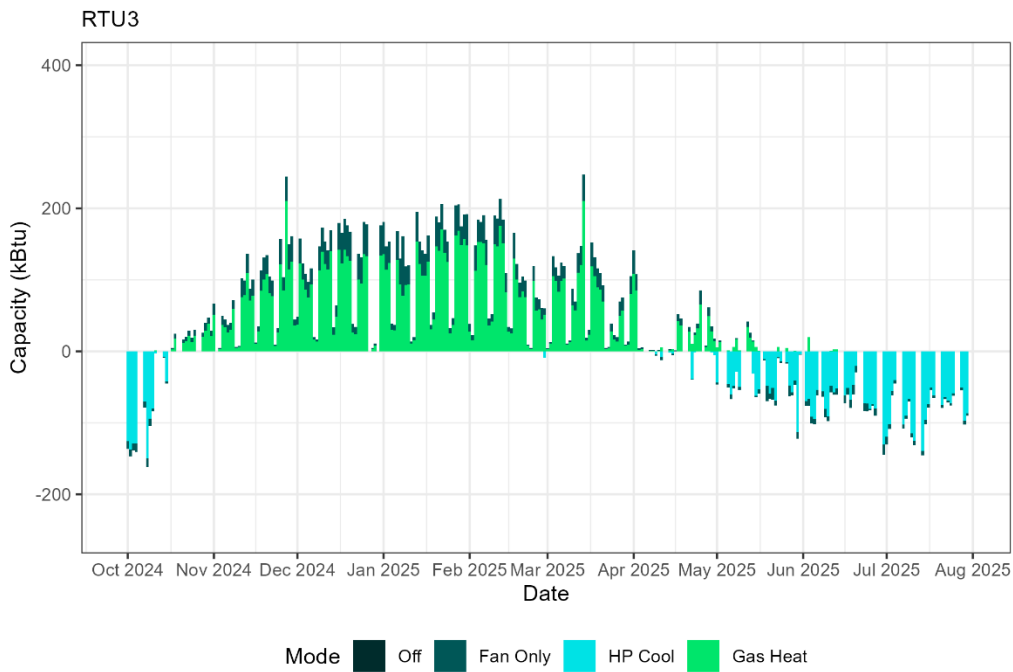


**Figure 24. Gas-Fired RTU - Net daily capacity delivered during the monitoring period**

### Overall COP by Outdoor Temperature Bin

Figure 25 shows the average overall COP for the RTUs at different outdoor ambient temperature conditions. This COP represents the total capacity delivered to the building by the RTU divided by the

total energy input over each 5-degree Fahrenheit temperature bin and accounts for energy used in all modes including Fan-Only and OFF. This plot shows a lower overall COP at very cold conditions when defrost occurs more frequently and compressor lift is highest. The COP improves as outdoor temperatures increase but then drops again when conditions become mild. The explanation for this is that there is very little capacity needed when conditions are mild causing the system to short-cycle and operate primarily in Fan-Only mode, reducing the calculated overall COP of the heat pump. Fan-only mode reduces the calculated overall COP since little or no capacity is delivered to the conditioned space while energy is used to provide ventilation. Similarly, in the cooling season, as outdoor air temperatures increase, there is a period when the COP improves followed by a reduction as temperatures become more extreme.

The overall COP is highest for the high-efficiency unit during the heating season with the exception of the mild temperature bins. The gas-fired RTU shows an overall COP below 1 since heating is provided through a natural gas furnace rather than a heat pump. During the cooling season, the standard efficiency RTU showed the highest COP values followed by the high-efficiency unit and gas-fired RTU. As mentioned previously, the overall COP accounts for all energy use including Fan-Only mode. It was observed that the standard efficiency RTU would operate its fan at a lower speed when in Fan-Only mode whereas the high-efficiency unit would operate at its full speed. This resulted in a fan energy consumption of ~260 Watts for the high-efficiency RTU versus ~146 Watts for the standard efficiency RTU. The difference in fan controls will impact the effective ventilation rate and the overall COP measured so this difference must be considered when comparing performance shown in Figure 26. The gas-fired unit was not set up to operate its fan for ventilation when not conditioning the building so this would also skew the result.

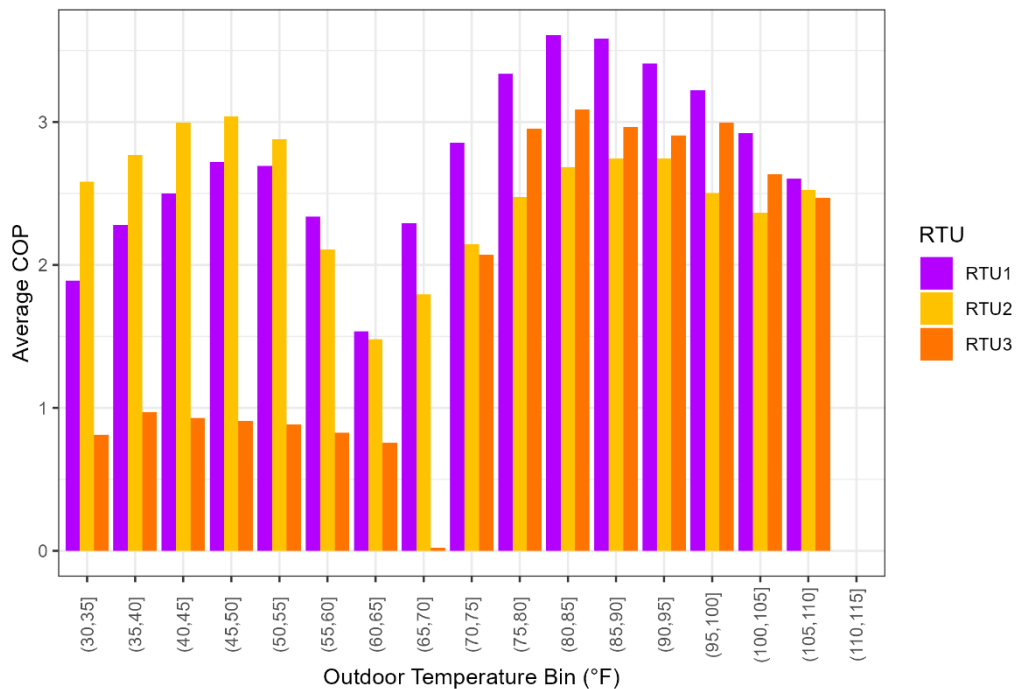


Figure 25. Standard HP RTU – Overall COP measured at different ambient temperature bins

## Mode-average COP by Outdoor Temperature Bin

Figure 26 shows the efficiencies measured for the RTUs during each mode of operation, including the fan operation immediately following the heating or cooling cycle. Points were excluded if they represented less than five hours of operation. The heating performance of the high-efficiency RTU was higher than the other units, but that RTU performed worst in cooling mode. Note that the inclusion of the post-heat operation of the fan brought the estimated COP for the gas-fired RTU close to 1.

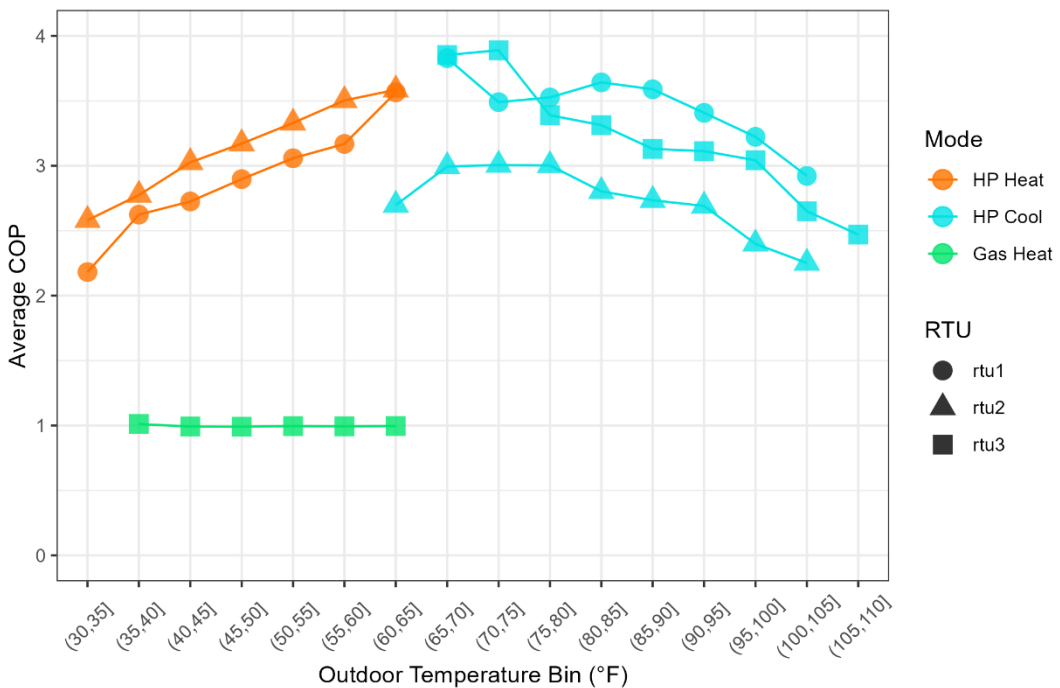


Figure 26. COP by mode and outdoor air temperature for each RTU

## Cycle-level Performance

The following sections summarize the performance of the systems in terms of their cycle characteristics. RTUs cycle on and off to maintain the desired indoor conditions because they are sized to provide sufficient heating and cooling in extreme design conditions and are unable to fully reduce their heating or cooling output to zero while remaining on. Data was aggregated for each temperature control cycle to calculate metrics including COP, duration, and final supply air temperature. A temperature control cycle was defined as beginning when the compressor or gas valve turned on and ending when those components turned off. Each unit cycled on and off thousands of times over the course of the monitoring period, so effectively visualizing the cycle-level performance requires plots that describe distributions instead of representing every data point directly.

## Cycle-average COP

Figure 27 shows the COP calculated for full compressor cycles. The COP calculated here only considers the efficiency while the compressor is on. The results show a relatively wide range of COP

with the majority of COPs in the range of 1-3. The standard efficiency RTU showed lower heating efficiency than the high-efficiency unit but similar cooling efficiency. Surprisingly, the gas-fired RTU showed slightly better cooling efficiency than the heat pump RTUs. This could be a result of the tradeoffs when optimizing a heat pump to perform efficiently in both heating and cooling modes. The measured efficiencies are also lower than one would expect based on the rated efficiency of the equipment, but again, these COP values only consider capacity delivered and energy used while the compressor was on, excluding any capacity delivered in the post-heating or post-cooling fan over-run period.

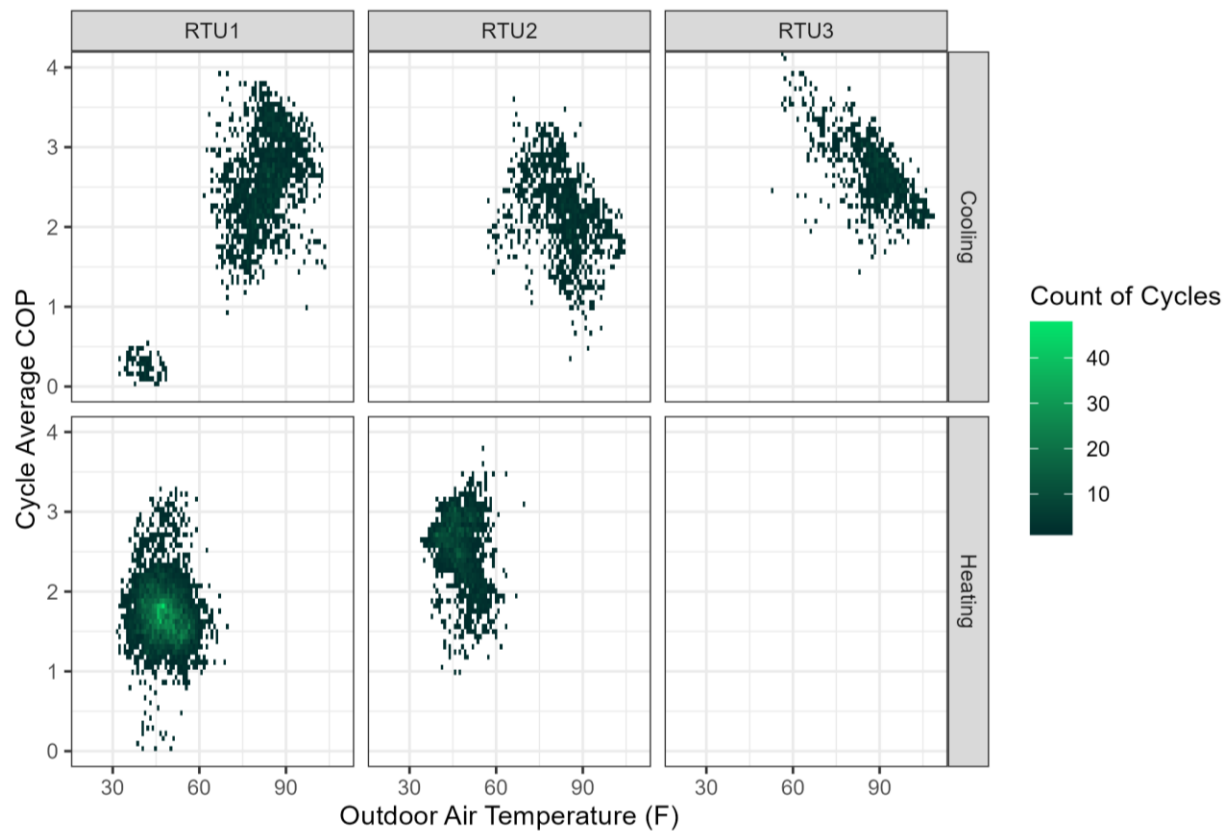


Figure 27. Average COP by compressor cycle at different outdoor air temperatures for each RTU

### Temperature Control Cycle Durations

Figure 28 shows boxplots describing heating and cooling cycle duration for each of the RTUs during the monitoring period plotted against the outdoor air temperature. The cycle duration for the high-efficiency unit is much longer since the compressor is capable of operating at part-load. In the coldest outdoor air temperature bin, the high-efficiency RTU would operate for an average of about 45 minutes per heating cycle compared to less than 10 minutes for the other two units. This behavior quickly changes after the coldest temperature bin showing a sharp decrease in average cycle times for the high efficiency unit. The cycle times for the high efficiency unit were still consistently longer than the other two units monitored.

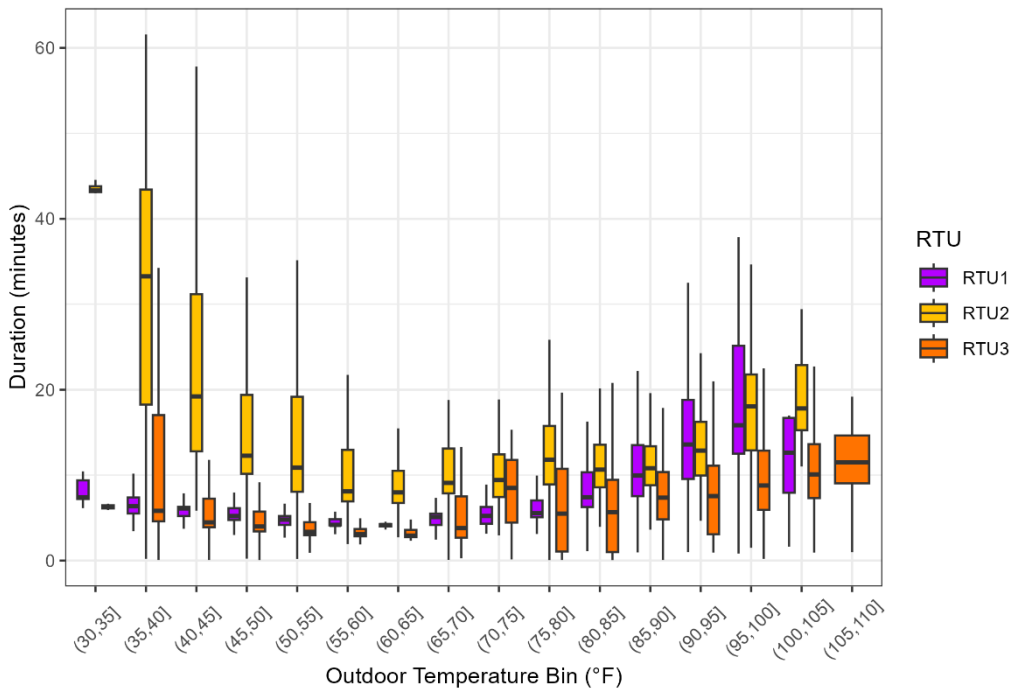


Figure 28. Heating and cooling cycle durations measured for each RTU

### Final Supply Air Temperatures in Heating Mode

Figure 29 shows the average supply air temperature measured at the end of a heating cycle representing the warmest delivery temperature of the unit under different outdoor conditions. The gas-fired RTU provides much warmer supply air temperatures often ranging between 125-155 °F compared to 85-105 °F for the heat pump RTUs. The high-efficiency RTU provided warmer supply air temperatures than the standard unit during cold outdoor conditions and a larger range of supply temperatures. Since the fans were operating at a constant speed, the supply air temperatures illustrate the decrease in capacity of the standard unit as outdoor temperatures decrease, whereas the high-efficiency unit can modulate the capacity by speeding up the compressor to adjust supply air temperature to buildings loads.

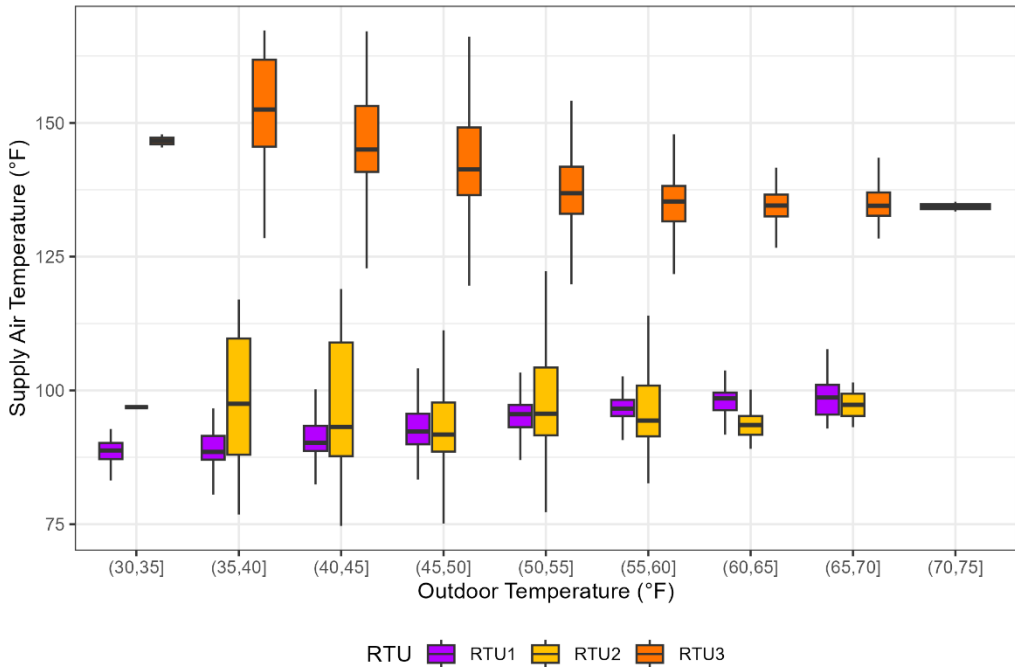
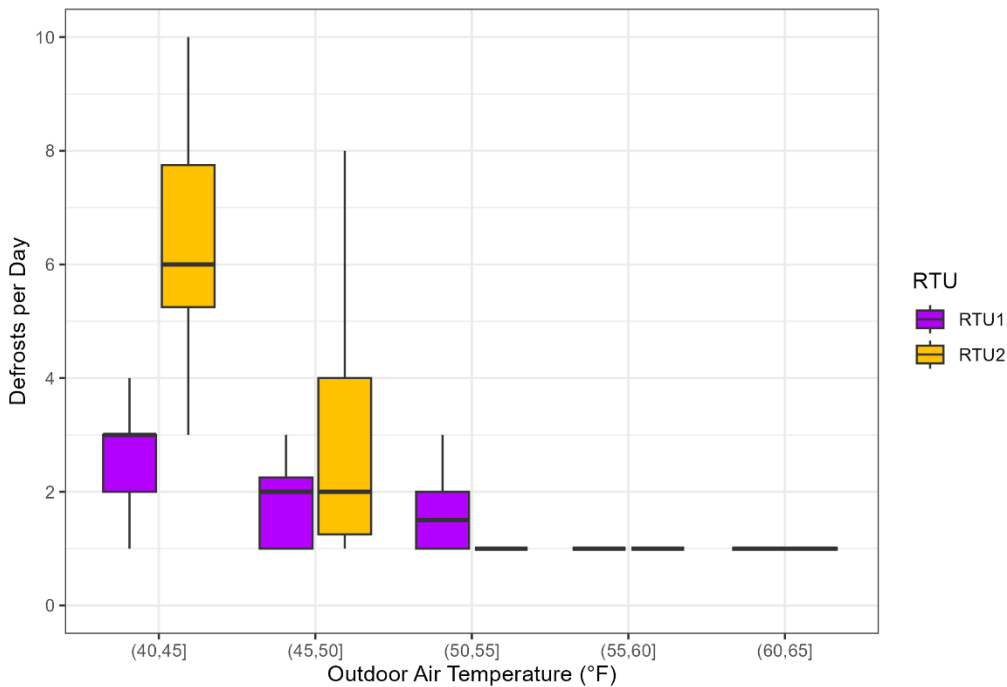


Figure 29. Final supply air temperatures in heating mode for all RTUs

### Defrosts Behavior

The heat pump RTUs exhibited very different defrost controls. The standard HP RTU used a reverse cycle (cooling mode) to heat the outdoor coil and melt the defrost while using the auxiliary electric resistance heater to re-heat the supply air to avoid overcooling the space. The defrost cycle for the standard unit is broken into two parts, the first part is the defrost cycle when the system operates in reverse cycle with simultaneous resistance heating, and the second part when the unit switches back to heat pump heating with simultaneous resistance heating. The high-efficiency HP RTU used a different approach which also relied on a reverse cycle to heat the outdoor coil but instead shut down the supply fan to avoid cooling the space. Figure 30 shows the number of defrost cycles performed each day at different daily average outdoor air temperatures for both HP RTUs. Both heat pumps performed more defrost cycles when temperatures were colder outside and avoided defrost at warmer outdoor air temperatures when coil icing would not be expected. The high-efficiency unit performed about three-times as many defrost cycles per day under the coldest conditions but achieved a similar number of cycles on average as temperature increased.



**Figure 30. Defrosts per day at different daily average outdoor air conditions for the heat pump RTUs**

Figure 31 and Figure 32 show the average time required for each defrost cycle showing a similar 2-4 minute duration for the reverse cycle period when the units operate in cooling mode to melt the ice on the coil. The standard efficiency unit exhibited an additional sequence after melting the ice which switched the unit back to heat pump heating mode while operating the electric resistance heater. This additional sequence was performed for nearly seven minutes on average after each defrost cycle. By contrast, the high-efficiency unit would simply switch to heat pump heating mode and modulate the indoor blower fan up to full speed at the end of each defrost cycle. The result is the standard unit defrost routine took place over an average of about nine minutes while the high-efficiency unit would defrost in four minutes.

### Defrost Event Duration

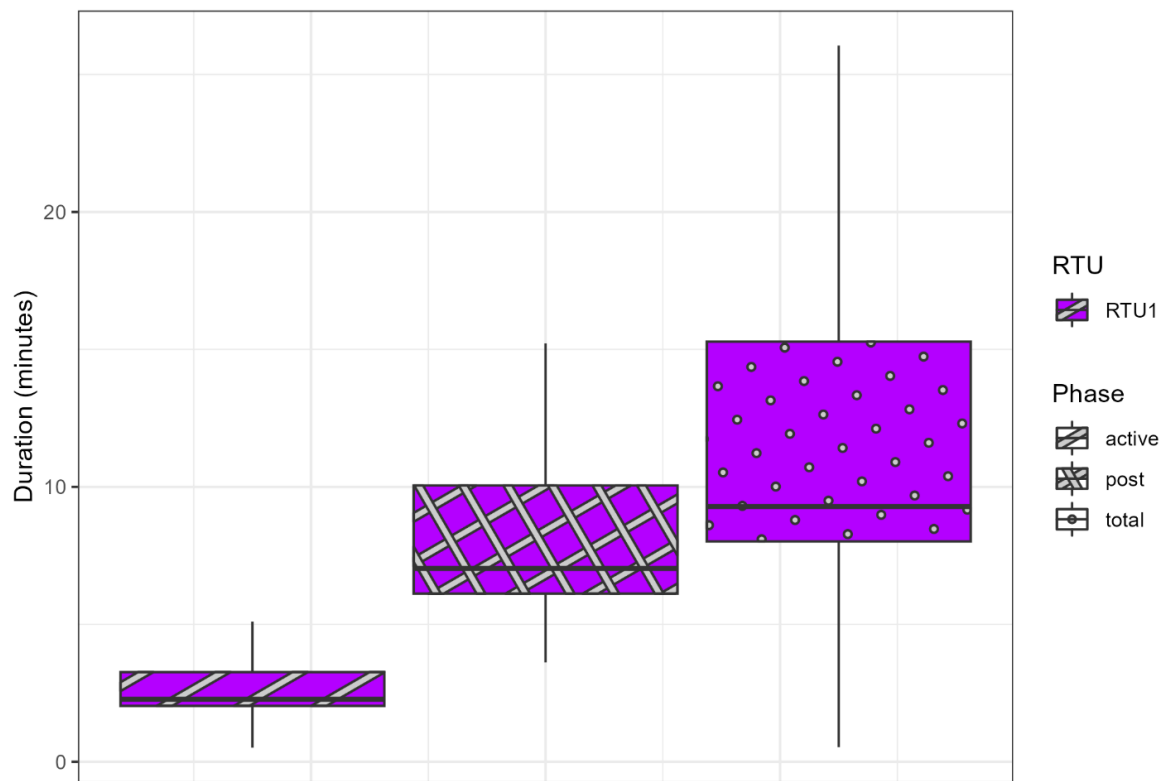


Figure 31. Standard HP RTU - Average defrost duration for each stage of the defrost cycle

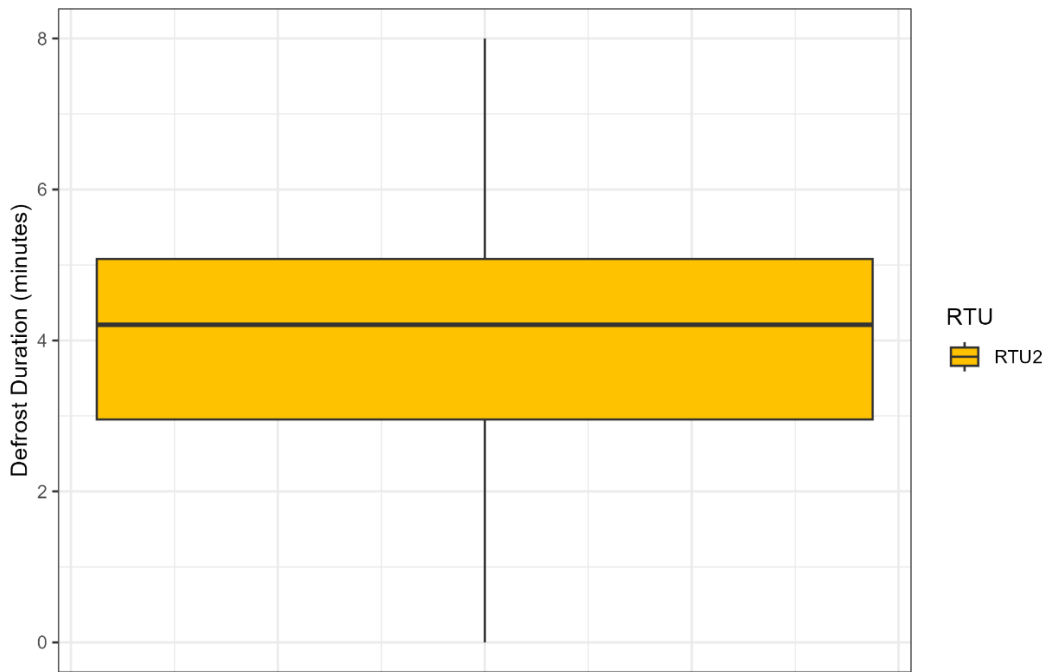


Figure 32. High-Efficiency HP RTU - Average defrost duration

When evaluating the defrost cycles, the goal is to understand the energy and comfort implications of the different approaches. The high-efficiency unit operating defrost more frequently but for a shorter amount of time while the standard unit would supplement the defrost with electric resistance heat to offset the cooling provided to the space during defrost. Figure 33 shows the average energy used during a defrost event for the two heat pump RTUs. The standard HP RTU shows significantly higher energy use due to the use of electric resistance heating with 0.5-1.3 kWh compared to less than 0.2 kWh for the high-efficiency unit. Furthermore, since the standard unit operates its blower fan during defrost there is a comfort impact due to the low supply air temperatures. Figure 34 shows the minimum supply air temperature measured for the standard unit during defrost cycles showing temperatures of 55-60 °F during defrost cycles in cold outdoor conditions. The high-efficiency unit avoids cooling the space by turning off the supply fan and heating the indoor coil before ramping up the supply fan at the end of a defrost cycle.

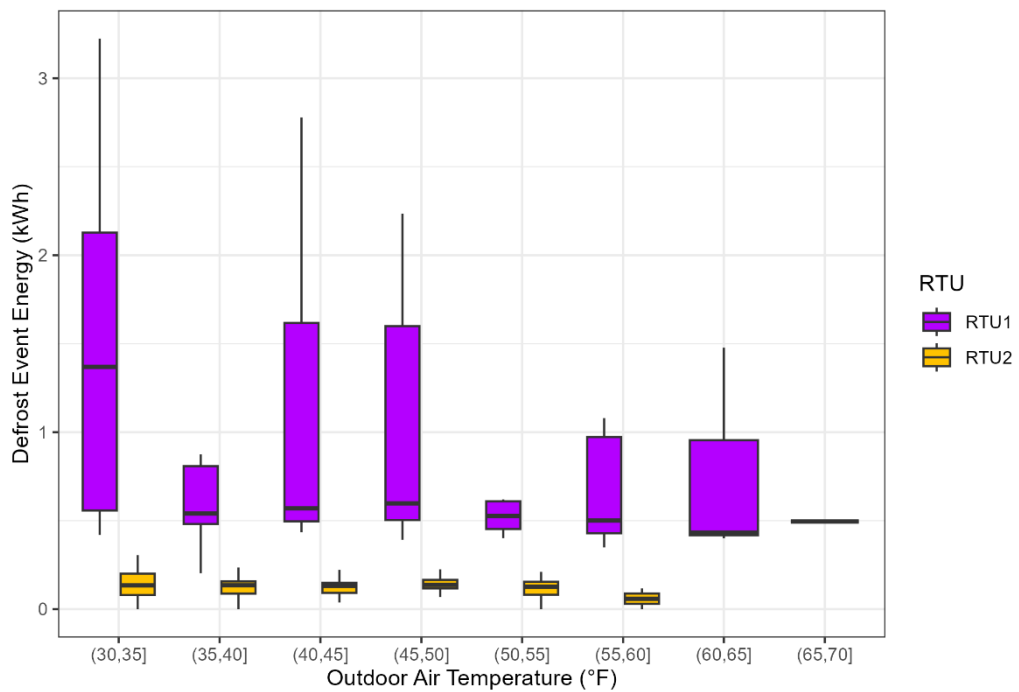


Figure 33. Defrost cycle energy use for the heat pump RTUs

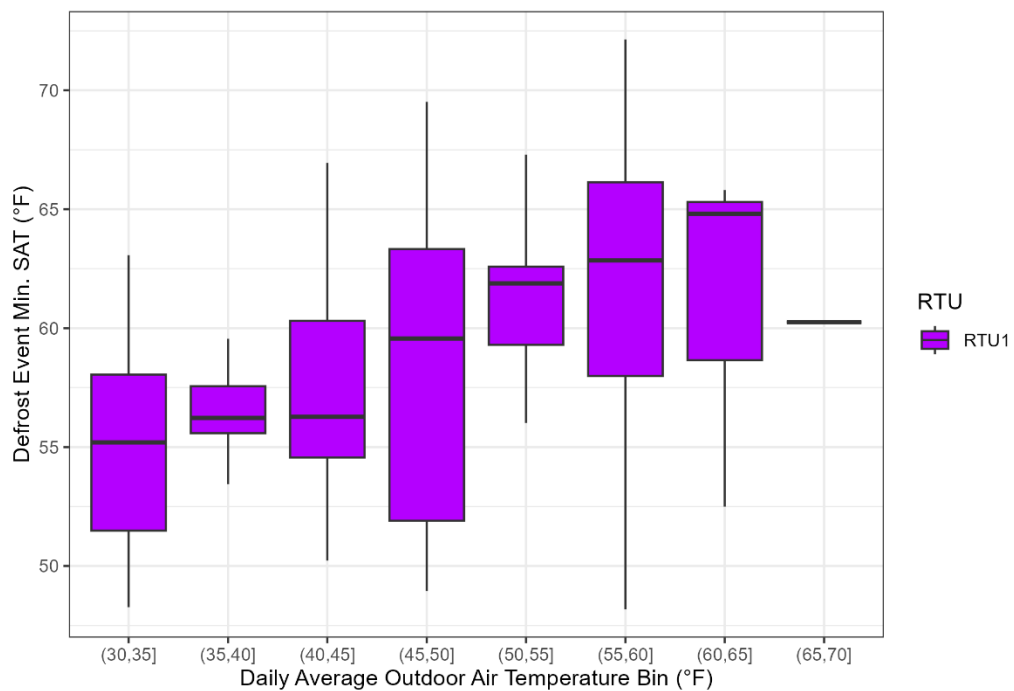


Figure 34. Standard HP RTU - Minimum supply air temperature measured during a defrost cycle

## Performance Modeling Results

Regression modeling was conducted to better compare the annual energy use and greenhouse gas emissions of each RTU. Table 10 and Table 11 provide statistics describing the accuracy of the regression models used in this analysis for both heating and cooling modes.

Table 10. Regression model statistics for heating

Heating	Measured Average COP	Modeled Average COP	R2	RMSE	Mean Abs Error %
RTU1	2.95	2.95	0.39	0.308	8%
RTU2	3.19	3.19	0.55	0.27	7%
RTU3	0.85	0.85	0.6	0.09	7%

Table 11. Regression model statistics for cooling

Cooling	Measured Average COP	Modeled Average COP	R2	RMSE	Mean Abs Error %
RTU1	2.73	2.73	0.55	0.3	8%
RTU2	2.69	2.69	0.56	0.39	12%
RTU3	2.45	2.45	0.55	0.27	9%

The results of this analysis are presented in Table 12 and show that the high-efficiency RTU had the lowest operating cost and lowest greenhouse gas emissions of the three units tested. The energy use and associated cost for the high-efficiency unit was about 7% lower than the other standard efficiency heat pump RTU representing a modest improvement. When evaluating the total energy used on site, the two heat pump RTUs showed over 50% reductions in energy use compared to the gas-fired unit. This does not translate directly into cost savings due to the differences in pricing structures for electricity and natural gas. The cost savings for the high efficiency heat pump RTU was about 10% compared to the gas-fired unit versus 3% for the standard efficiency heat pump compared to the gas-fired unit. The difference in on-site energy use is more apparent when evaluating the greenhouse gas emissions reductions of the heat pump RTUs compared to the gas-fired unit. The greenhouse gas emissions were reduced by 60-68% for the heat pump RTUs compared to the RTU with a gas furnace.

Table 12. Normalized energy use for each RTU operating at the RTU1 site

	Electricity [kWh]			Gas [Therms]		
	RTU1	RTU2	RTU3	RTU1	RTU2	RTU3
Heating	2210	1956	343	0	0	260
Cooling	3164	3049	3280	0	0	0
Total	5374	5005	3623	0	0	260

	Cost			Emissions [lb CO2e]		
	RTU1	RTU2	RTU3	RTU1	RTU2	RTU3
Heating	\$508	\$450	\$521	1681	1462	3300
Cooling	\$728	\$701	\$754	1214	1080	1210
Total	\$1,236	\$1,151	\$1,275	2895	2542	4510

## Stakeholder Feedback

The project team has reached out to various stakeholders over the course of the project including manufacturers, contractors, CalNEXT project partners, CalIMTA, and other subject matter experts. There is a keen interest in developing a better understanding of the heat pump RTU market in California, specifically related barriers to adoption and cost implications.

### Manufacturers

Discussions with manufacturers have been focused on heat pump RTU development and emerging technologies. These discussions highlighted some of the considerations for adding supplemental electric resistance heat to RTUs used in commercial applications. One concern is that heat pumps generally have lower capacity than the furnace systems they replace causing the supply air temperature to be lower than natural gas systems. This effect has been referred to as “cold blow” by consumers and can impact the comfort of the occupants. In commercial applications, ventilation air is often introduced by adding outdoor air into the return flow path which causes the mixed air condition (condition of air entering the heat pump coil) in the winter to be colder. This can exacerbate the issue of “cold blow”, especially during very cold weather conditions. It is expected that variable capacity systems can counter this by adjusting airflow rate and compressor speed to optimize supply air temperature conditions. This project did not identify any specific issues related to supply air temperature and there was no concern expressed by the building occupants relative to this issue.

### Contractors

Contractors have noted that the installation of heat pump RTUs is similar to other RTU products but often include electrical upgrades to support supplemental electric resistance heat. If electric resistance heat is not included in the installation, the process would be similar to replacing a conventional gas RTU with the new unit using the existing circuit for the RTU, or potential easier since routing the gas line for the new unit can require additional work and there is no need to adjust the fan speed for furnace heating. There are many examples of contractors installing heat pumps without electric resistance heat in California. Other aspects of the installation were similar to installing a conventional unit including the use of a curb adapter for mounting the new unit on the roof curb. These curb adapters are usually supplied by a 3<sup>rd</sup> party contractor that works with the

equipment vendor. There can also be proprietary communication protocols for variable-capacity systems that complicate integration into existing building management systems. Testing and balancing efforts are rarely performed when retrofit equipment is replacing a unit with comparable airflow requirements.

### **CalMTA**

The California Market Transformation Administrator (CalMTA) has expressed interest in the results of this technology evaluation to inform their work on the topic of heat pump RTUs. CalMTA has developed a market transformation initiative around efficient rooftop units (ERTUs). CalMTA plans to use this research to help support the development of key features for ERTUs, identify potential market barriers, and develop recommendations for addressing market barriers. CalMTA also funded a follow-on study to evaluate energy efficiency features of high-efficiency RTUs including variable speed compressors and fans, and real-time monitoring systems.

### **Subject Matter Experts**

The team has also discussed this project with other researchers and subject matter experts in the area of heat pump RTUs. We reached out to the DOE Commercial Heat Pump Accelerator about their experience installing heat pump RTUs on Los Angeles Unified School District campuses. They noted that electrical capacity was often adequate to support the heat pump installation, and that electric resistance heating is not necessary in the Los Angeles climate. They also found that schedules had to be adjusted to start the heat earlier in the morning because of the longer heat-up times. Center for Energy and Environment has primarily studied the performance of heat pump rooftop units in cold climates where supplemental heat is necessary to maintain acceptable indoor conditions. This project was interesting from their perspective because it highlighted the performance differences between two different types of heat pump RTU in nearly identical applications that generally did not require supplemental heat. The findings from this study built on findings from previous studies showing that implementations of control algorithms governing heat pump heating, defrost, and supplemental heat vary by RTU. Evaluations such as this help to tailor heat pump RTU equipment recommendations depending on the end users' specific priorities for comfort, as well as capital cost, operating cost, and emissions savings.

## **Conclusions and Recommendations**

This project evaluated the performance of multiple RTU products installed on commercial office buildings to better understand the benefits and potential barriers for heat pump RTU installations in California. Two heat pump RTUs with different rated efficiencies were installed and compared to an existing RTU that used a natural gas furnace for heating. Data was collected on the systems during both heating and cooling seasons from October 2024-June 2025. The high-efficiency heat pump RTU utilized a variable-speed compressor for achieving better performance at part load while the standard-efficiency heat pump RTU used a single-speed compressor.

The results showed that the high-efficiency RTU reduced heating and cooling energy consumption by 7% relative to the standard-efficiency RTU which is lower than expected considering the rated efficiency was 25% higher for the high-efficiency unit. This result was partly caused by the way the high-efficiency unit was commissioned to operate its fan, which was set at full speed whenever the

building was occupied to ensure ventilation rates were maintained. This meant that the unit was not allowed to modulate the fan speed down when operating in part load which is how the unit would operate during the rated testing. This observation highlights the challenge associated with realizing the energy savings of variable-speed supply fans in commercial applications. It is common for outdoor air dampers to be set at a fixed position based on the minimum ventilation needed for a building when the fan is operating at full speed. Therefore, the fan must operate at full speed to achieve the intended ventilation rate. Demand control ventilation strategies could improve this, but those controls tend to only modulate the outdoor air damper without changing the fan speed.

The largest difference in operation between the high-efficiency and standard-efficiency heat pump RTUs was related to their defrost strategy and peak power draw. The high-efficiency RTU did not include any electric resistance auxiliary heating while the standard-efficiency RTU included a 5kW heating element. Defrost controls for the high-efficiency RTU allowed the unit to perform defrost with the supply fan off by making use of the modulating compressor. This prevented the unit from delivering cold air to the building during defrost, improving comfort. The standard-efficiency RTU used a more traditional approach where the unit would enter cooling mode and use the electric resistance heater to reheat that air before entering the space. Supply air temperatures for the standard heat pump showed temperatures as cold as 55 °F during a defrost cycle which would impact occupant comfort and add heating load to the building. The high-efficiency unit went into defrost mode more frequently but overall was able to perform defrost using less energy than the standard unit. Defrost cycles also represented the highest peak load for the standard RTU with peak power draw more than double the high-efficiency unit at over 7 kW. Commercial utility rates often include a cost associated with peak power consumption which means this additional power draw could have a large impact on utility costs for commercial building owners.

When comparing the performance between the heat pump RTUs and the gas-fired RTU, the heat pump units demonstrated significant potential to reduce energy use and greenhouse gas emissions. Both heat pump RTUs showed reduction in on-site energy use and greenhouse gas emissions of more than 50% compared to the gas-fired RTU. The cost savings for the high efficiency heat pump RTU was about 10% compared to the gas-fired unit versus 3% for the standard efficiency heat pump compared to the gas-fired unit showing a cost benefit to ratepayers even when the relative cost of natural gas is low compared to electricity.

The results of this project show the overall benefit of heat pump RTUs over gas-fired RTUs. Both heat pump RTUs tested resulted in lower utility costs and substantially lower greenhouse gas emissions compared to the gas unit. The high-efficiency RTU had the lowest energy cost and was able to provide comfort without the use of electric resistance auxiliary heaters. This resulted in lower peak power draw compared to the standard heat pump RTU. Evaluating the 15-minute peak power draw of both HP RTUs showed a 20% reduction in the winter for the high-efficiency unit without electric resistance heaters. In addition, eliminating the electric resistance heater is expected to reduce cost barriers associated with heat pump RTU retrofits by avoiding the need to upgrade electrical service to the location of the RTU, and avoiding larger barriers associated with potential panel upgrades to support heat pump retrofits.

## References

SCE (2015). *Laboratory and Field Testing of RTU Optimization Package Combining a Condenser-Air Pre-Cooler with Compressor Speed Reduction*. Southern California Edison Emerging Products ET15SCE7030